

Analysis of a Heavy Lift Launch Vehicle Design Using Small Liquid Rocket Engines

by

DAVID PHILLIP RUSS

S.B., Massachusetts Institute of Technology
1987

SUBMITTED IN PARTIAL FULFILLMENT
OF THE REQUIREMENTS FOR THE
DEGREE OF

MASTER OF SCIENCE IN
AERONAUTICS AND ASTRONAUTICS

at the

MASSACHUSETTS INSTITUTE OF TECHNOLOGY

May 1988

© David P. Russ 1988

The author hereby grants M.I.T. and Hughes Aircraft Company permission to reproduce and to distribute copies of this thesis document in whole or in part.

Signature of Author _____
Department of Aeronautics and Astronautics
December 18, 1987

Reviewed by _____
C. P. Rubin
Hughes Aircraft Company

Certified by _____
Professor Walter M. Hollister
Thesis Supervisor, Department of Aeronautics and Astronautics

Accepted by _____
Professor Harold Y. Wachman
Chairman, Departmental Graduate Committee
Department of Aeronautics and Astronautics

MASSACHUSETTS INSTITUTE
OF TECHNOLOGY

MAY 24 1988

LIBRARIES

Aero

WITHDRAWN
M.I.T.
LIBRARIES

Analysis of a Heavy Lift Launch Vehicle Design Using Small Liquid Rocket Engines

by

David P. Russ

Submitted to the Department of Aeronautics and Astronautics

in partial fulfillment of the requirements for the degree of

Master of Science in Aeronautics and Astronautics

May, 1988

Abstract

The trend in launch vehicle design has been to increase performance by using engines of greater and greater complexity, which has a negative effect on cost and reliability. However, a design making use of over 300 small, simple rocket engines can deliver over 340,000 lbs to low Earth orbit. This design, derived by using the rocket equations to size the major components, features a 42 ft. diameter core with 78 engines and eight 26 ft diameter strap-ons with 30 engines apiece. The amount of payload carried by this design is maximized by varying five vehicle parameters and selecting values which maximize payload within constraints. Next, a number of externally determined parameters are varied to study the variation in payload if these parameters have unexpected or non-optimal values. The payload capacity is most sensitive to changes in specific impulse and mass fraction; the variation of payload with acceleration limit and number of strap-ons shows the design to be quite flexible. The problem of in-flight engine failure is analyzed with respect to payload capacity, control authority, and propellant management, and methods of dealing with this problem are discussed. The result is a flexible, reliable, and very capable design.

Thesis Supervisor: Walter M. Hollister

Professor of Aeronautics and Astronautics

Preface

The idea for using a large number of small, simple liquid rocket engines for a heavy-lift launch vehicle is not original to the author. As near as I can tell, the idea came from Paul Visher, a vice president with Space and Communications Group of Hughes Aircraft. This has formed the basis for a whole new enterprise for Hughes: launch vehicle design. The design presented below is sufficiently different from the Hughes design so that it does not infringe on any proprietary data, but it does share most of the key advantages of the Hughes concept.

The author would like to thank the following people and institutions for their invaluable support.

- MIT, and especially Professor Hollister and John Martucelli, director of the Engineering Internship Program. The EIP placed me here, and I am deeply grateful.
- The staff of the Hughes Co-op Office (especially Mimi Shefrin) and Dr. John Drebing. They, too, have provided key support.
- Chuck Rubin and Dave Knauer, the leaders of the current Hughes launch vehicle effort. They have trusted me enough to give me an interesting position.
- My family—mother, father, and brother—who looked at early drafts and provided moral support. They, and the faith in God that they helped to impart, have kept me going.

El Segundo, CA

December, 1987

Contents

1	Introduction	6
2	Concept Definition	8
2.1	Reference Mission	8
2.2	Propulsive Capacity	8
2.2.1	Actual ΔV	9
2.2.2	Drag ΔV	10
2.2.3	Gravity ΔV	12
2.3	Rocket Equations	13
2.4	Initial Design	15
2.4.1	Engine Selection	15
2.4.2	Strap-on Design	15
2.4.3	Propellant Tanks	20
3	Performance Analysis	27
3.1	Performance Analysis Background	27
3.1.1	The Trajectory Simulator	27
3.1.2	Vehicle Assumptions	28
3.1.3	Analysis Methodology	32
3.2	Trade Studies	32
3.2.1	Liftoff Weight	32

3.2.2	Core/Strap-on Size Ratio	34
3.2.3	Core/Strap-on Engine Ratio	36
3.2.4	Acceleration Limit	38
3.2.5	Core Shutdown Time	40
3.2.6	Trade Study Summary	42
3.3	Variation Studies	42
3.3.1	Mass Fraction	42
3.3.2	Drag	43
3.3.3	Number of Strap-ons	45
3.3.4	Specific Impulse	47
3.3.5	Variation Study Summary	47
3.4	Trajectory Description	49
4	Engine Failure	57
4.1	Overview	57
4.2	Payload Capability	58
4.3	Control	60
4.3.1	Nominal Control	60
4.3.2	Control with Failed Engines	62
4.3.3	Control Summary	64
4.4	Propellant Consumption Management	65
4.5	Engine Failure Summary	66
5	Conclusion	68
	Bibliography	70

Chapter 1

Introduction

The problems of getting payload from the Earth's surface into space have intrigued many people during the course of the 20th century. The past 30 years have seen advancement in this field that is more rapid than most other technological fields. Launch vehicles are now available that can place tens of thousands of pounds into low Earth orbit (LEO) and thousands of pounds into geosynchronous Earth orbit (GEO). The two major problems with such vehicles continue to be cost and reliability. There is no other form of transportation that costs thousands of dollars per pound delivered; modern launch vehicles have costs that are the equivalent of mailing a letter for \$250¹. And tremendous reliability is required since the payloads themselves may be worth millions or billions of dollars.

One key area of booster design is engine selection. The choice of engines affects the performance, cost, and reliability of a launch vehicle in a fundamental way. Up until now, the main focus of engine development has been to develop engines that have great performance. The Space Shuttle Main Engines (SSME's) are a prime example of this. They have a specific impulse (I_{sp}) of 455 seconds in a vacuum, among the highest ever achieved by a rocket engine, and are capable of producing 375,000 pounds (1,670,000 N) of thrust apiece at sea level [1, page A-53]. But,

¹Based on a launch cost of \$4000/lb for the Titan IV and a one ounce letter.

they are extremely expensive and can only be flown for a few flights before a major overhaul. Even with this expense, an engine was shut down in flight.

Thus one item that is needed to build a low-cost heavy lift launch vehicle is a low-cost, reliable engine of good performance. An example of this is the RL10, developed by Pratt and Whitney and currently used on the Centaur upper stage. This engine has a vacuum I_{sp} of 440 sec. and has had *no* in-flight failures in 220 flight firings [2]. The engine is simple, with a complexity similar to that of a helicopter turbine engine. The only drawback is that this engine produces 15,000 lbs (67,000 N) of thrust at sea level; in other words, an average launch vehicle would need around 50 such engines to get off of the ground. Ignoring this drawback for a moment, the demonstrated reliability of 0.9984 and the possibility of mass production force one to consider a design based on this engine.

The purpose of this thesis is to generate a design using an uprated version of this engine, improve the payload capacity by varying many of its parameters, and address one of the major technical problems with this design, engine failure. This design could offer a major improvement in launch cost and performance.

Chapter 2

Concept Definition

2.1 Reference Mission

The design presented here is that of a heavy lift launch vehicle. The reference mission, then, will be to take 300,000 lbs (136,000 kg) to a circular low Earth orbit (LEO) at 100 nautical miles (185 km) altitude based on a due east launch from Kennedy Space Center. The first step is to use the rocket equations to calculate the amount of propellant needed. These equations, in turn, require knowledge of the amount of propulsive ΔV the launch vehicle must provide.

2.2 Propulsive Capacity

Consider the dynamics of a vehicle in flight at velocity \vec{u} at an angle γ to the local horizontal, as in figure 2.1. The vehicle has mass m , produces a thrust \vec{T} with a certain specific impulse (I_{sp}), and experiences a drag \vec{D} .

These forces can be expressed in the following equation [3, page 323]:

$$du = -gI_{sp}\frac{dm}{m} - \frac{D}{m}dt - g \sin \gamma dt \quad (2.1)$$

where T and D represent the magnitude of these forces resolved in the \vec{u} direction.

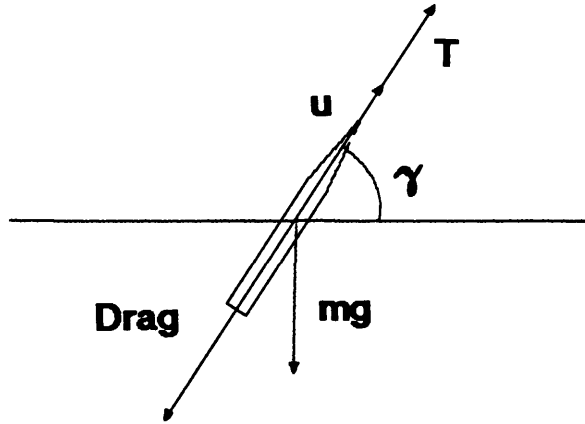


Figure 2.1: The forces on a launch vehicle in flight. T is the thrust as resolved in the u direction.

There are four terms present. When integrated, they represent the actual change in velocity (ΔV_a), the propulsive change in velocity (ΔV_p), the change in velocity due to drag (ΔV_D), and the change in velocity due to gravity (ΔV_G). The integration of each term is complicated, but the integrated form can be thought of as follows:

$$\Delta V_a + \Delta V_D + \Delta V_G = \Delta V_p \quad (2.2)$$

Use of the rocket equations to size the vehicle will require evaluating each of these terms.

2.2.1 Actual ΔV

The actual ΔV is the difference between the inertial velocity of the vehicle at rest on a rotating Earth and the inertial velocity of the vehicle at burnout in orbit. To first order, this can be approximated by calculating the orbital velocity required (V_{orb}) and subtracting from it the Earth's rotational speed at the latitude of the launch site (V_{Earth}).

V_{orb} , for low Earth orbit, is found as follows [4, page 126] :

$$V_{orb} = \sqrt{\mu \left(\frac{2}{r} - \frac{1}{a} \right)} \quad (2.3)$$

where μ is $G \cdot m_{Earth}$, the gravitational constant times the mass of the Earth, r is the distance of the body in orbit from the center of the Earth, and a is the semi-major axis of the orbit.

For a circular orbit, $r = a$, and assuming the body is at 185 km altitude,

$$V_{orb} = \sqrt{398601 \cdot \left(\frac{1}{6378 + 185}\right)} = 7793 \text{ m/sec}$$

or 25,570 ft/sec.

V_{Earth} at the equator is found as follows:

$$V_{Earth} = \frac{2\pi r}{t} = \frac{2 \cdot \pi \cdot 6378}{24 \cdot 60 \cdot 60} = 464 \text{ m/sec} \quad (2.4)$$

or 1520 ft/sec. At other latitudes, this is reduced by a cosine factor. The latitude of Kennedy Space Center is 28.5° , giving

$$V_{Earth} = 464 \cos L = 464 \cos(28.5) = 408 \text{ m/sec}$$

or 1340 ft/sec.

Thus, ΔV_a is approximately 7385 m/sec or 24,230 ft/sec.

2.2.2 Drag ΔV

By definition, drag acts along the direction of the relative airspeed of the launch vehicle. Its magnitude is found as follows:

$$D = \frac{1}{2} \rho v^2 C_D A_{ref} \quad (2.5)$$

where ρ is the local atmospheric density, v is the airspeed, C_D is the coefficient of drag, and A_{ref} is the reference area. The grouping $\frac{1}{2} \rho v^2$ is sometimes referred to as q , the dynamic pressure.

This force, when divided by the mass and integrated over time gives the drag loss as follows.

$$\Delta V_D = \int_0^{t_b} \frac{D(t)}{m(t)} dt \quad (2.6)$$

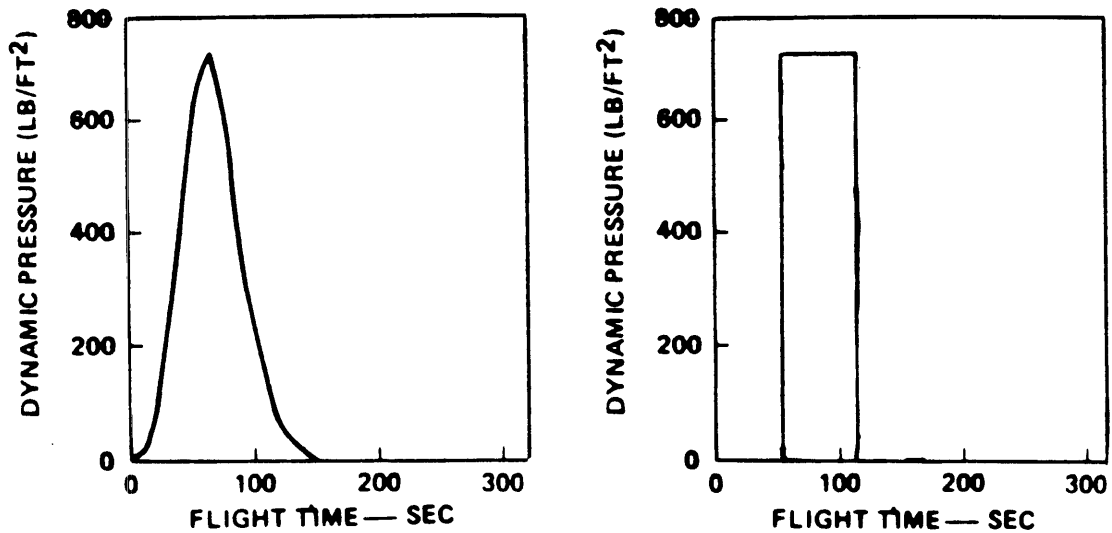


Figure 2.2: The first graph is dynamic pressure versus time for another heavy lift launch vehicle. The second shows an approximation to this.

where t_b is the burn time.

Needless to say, this integral is too complicated to evaluate, especially when one does not have a design yet. However, one can approximate the effect of drag by calculating the peak drag acceleration and assuming that this acceleration is a constant for some period of time. Shown in figure 2.2a is a typical curve for the dynamic pressure of a launch vehicle as a function of time [5, page 81]. To first order, the dynamic pressure can be approximated as in the second graph. The maximum value of q is about 730 lbs/ft² (35,000 N/m²), and this is the equivalent of lasting for 50 seconds. C_D is unknown, but in the atmosphere, it is of the order of 1. Assume that the vehicle has an area equal to 10 times that of the shuttle external tank, or 5940 ft² (552 m²). The mass is also unknown, but, scaling up from the space shuttle during the period when drag is near its maximum, it will be of the order of 4,400,000 lbs (2,000,000 kg). This gives (in metric units)

$$\Delta V_D = \frac{35000 \cdot 1 \cdot 552}{2000000} \cdot 50 = 500 \text{ m/sec}$$

or 1600 ft/sec.

2.2.3 Gravity ΔV

For a short thrust period t , and neglecting drag, one can integrate equation 2.1 to obtain [3, page 324]:

$$\Delta V_G = g t \sin \gamma$$

Over the course of a flight of duration t_b , this can be approximated as

$$\Delta V_G \approx g t_b \overline{\sin \gamma} \quad (2.7)$$

where $\overline{\sin \gamma}$ is the integrated average value of $\sin \gamma$ over the burn.

This $\overline{\sin \gamma}$ has some physical meaning. To first order, it is the time averaged value of $\sin \gamma$, where γ is as defined in figure 2.1. Launch vehicles launch straight upward ($\gamma = 90^\circ$) initially. When in a circular orbit, $\gamma = 0^\circ$. Assuming that the launch vehicle pitches over as soon as possible so as to minimize g losses, more time is spent at lower values of γ . 30° is a reasonable estimate.

t_b is approximated as follows:

$$t_b = \frac{m_{prop}}{\dot{m}} \quad (2.8)$$

where m_{prop} is the propellant mass and \dot{m} is the mass flow rate. Given that T is the thrust and I_{sp} is the specific impulse, and using the definition of specific impulse, one obtains

$$I_{sp} = \frac{T}{\dot{m}g} = \frac{T t_b}{m_{prop}g} \quad (2.9)$$

To stay in the air, $T \geq m_{prop}g$, so $t_b \leq I_{sp}$ for any single stage. For a two stage vehicle, each stage having $t_b = \frac{1}{2}I_{sp}$, this gives $t_b = I_{sp}$ overall. The overall I_{sp} of the liquid hydrogen/liquid oxygen propulsion is around 400 sec., giving

$$\Delta V_G = 9.8 \cdot 400 \cdot \sin 30^\circ = 1960 \text{ m/sec}$$

or 6430 ft/sec.

Thus, the approximations above lead to

$$\Delta V_p = 7385 + 500 + 1960 = 9850 \text{ m/sec} = 32,300 \text{ ft/sec} \quad (2.10)$$

This propulsive ΔV is used in the rocket equations to size the vehicle.

2.3 Rocket Equations

The mass of a launch vehicle can be broken up into three categories [3, page 328]:

m_{pay} , the mass of the payload,

m_{prop} , the mass of the propellant burned, and

m_{struc} , the mass of the structure and everything else (e.g., residual propellant, avionics, etc.).

The sum of these is m_0 , the total liftoff mass. There are two ratios, defined as follows:

$$\mathcal{R} = \frac{m_{pay}}{m_{pay} + m_{prop} + m_{struc}} = \frac{m_{pay}}{m_0} \quad (2.11)$$

$$\varepsilon = \frac{m_{struc}}{m_{struc} + m_{prop}} \quad (2.12)$$

The ratio ε is referred to as the mass fraction.

In addition, define the exponent k as follows:

$$k = \frac{\Delta V_p}{cn} \quad (2.13)$$

where c is gI_{sp} for each stage and n is the number of stages.

For the entire vehicle (assuming stages of equal I_{sp} and ε) [3, page 333]

$$\frac{\Delta V_p}{c} = n \ln \left[\frac{(1/\mathcal{R})^{1/n}}{\varepsilon[(1/\mathcal{R})^{1/n} - 1] + 1} \right]$$

This can be solved for $\frac{1}{\mathcal{R}}$ as follows:

$$\frac{1}{\mathcal{R}} = \left(\frac{e^k (1 - \varepsilon)}{1 - \varepsilon e^k} \right)^n \quad (2.14)$$

ΔV_p is known to be 9850 m/sec from above. ε is unknown, but is of the order of 0.1 [3, page 329]¹. This formula allows one to calculate the inverse of the mass ratio

¹The graph in Hill shows that 0.05 is a good estimate, so 0.1 is conservative.

I_{sp} (sec.)	Number of stages		
	1	2	3
400	∞	23.7	19.8
350	∞	42.5	31.8
300	∞	106.0	61.9

Table 2.1: $\frac{1}{\mathcal{R}}$ for several scenarios.

($\frac{1}{\mathcal{R}}$) for a range of I_{sp} and number of stages². This is shown in table 2.1. Given the desired payload mass, the liftoff mass of the vehicle is found directly. Clearly, the smaller this number, the smaller the overall vehicle. (The I_{sp} is the overall average I_{sp} from sea level to vacuum. A one-stage vehicle with strap-ons would be considered a two-stage vehicle.)

An I_{sp} of 300 seconds corresponds to that of a vehicle that makes much use of solid or non-cryogenic motors, which tend to have lower I_{sp} . The vehicle under consideration would have an average I_{sp} of 400 seconds. One can see the motivation of using an all-liquid propulsion system, as the higher I_{sp} results in a much lower total liftoff weight. Note further that there is little benefit for having a third stage; the numbers above show only a 15% loss in liftoff weight for a 50% gain in the number of stages. The next question is whether to have two stages that fire in series or have a core with strap-ons. Since the vehicle must have enough thrust to leave the ground, and since the engines providing this thrust are small, it is best to have as many engines as possible firing at liftoff. Thus, a good baseline is a one-stage core vehicle with strap-ons. The analysis above also yields the size. For a m_{pay} of 300,000 lbs, m_0 must be $23.7 \cdot 300000$ or 7,110,000 lbs. Using ϵ as defined above,

²The analysis for ΔV_p assumed two stages, but the result is only weakly dependent on this number, as it appears only in the gravity loss term.

this gives a structural mass of 681,000 lbs and a propellant mass of 6,129,000 lbs.

2.4 Initial Design

2.4.1 Engine Selection

Obviously, a major constraint on launch vehicles is that they must get off the ground. In numeric terms, this means that the thrust must be greater than the weight. Let us assume that the thrust to weight ratio is 1.2 at liftoff, giving a takeoff thrust of 8,532,000 lbs at sea level. Regardless of the choice of small thrust engine, one is going to need hundreds of engines firing at liftoff. If the engines have a thrust of 10,000 lbs apiece, one will need 854 engines; even if the thrust is as great as 100,000 lbs, one will still need 86 engines.

The aforementioned RL10 has a vacuum thrust around 16,500 lbs (73,400 N). However, Pratt and Whitney has conducted a study which concluded that this engine can easily be uprated to 27,000 lbs (120,100 N) of sea level thrust while maintaining the simplicity needed for mass production [2]. This engine, referred to as the RL10J, will be used as the baseline engine for this design. Liftoff would require at least 316 such engines.

An efficient scheme for mounting these engines is to mount the engines in clusters. From the standpoint of controls and plumbing, each cluster can be treated as a single engine. The RL10 has flown in clusters of 6 on early versions of the S-IV stage, so the engines in this design will be mounted in clusters of 6. Thus, the initial design will rely on 318 RL10J engines.

2.4.2 Strap-on Design

There are a number of possibilities for strap-on size and engine placement. For each possibility, there are ways of using the same design with fewer than the maximum possible number of strap-ons. For example, if one had an eight strap-on design,

Maximum Number of Strap-ons	Alternate Configurations
2	0,2
4	0,2,4
6	0,2,3,4,6
8	0,2,4,6,8
9	0,3,6,9

Table 2.2: Possible alternate configurations that use fewer than the maximum number of strap-ons while maintaining symmetry.

one could remove an opposing pair of strap-ons and have a symmetric six strap-on configuration. But, in this example, removal of an odd number of strap-ons is not possible because this would result in asymmetric thrust. All of the possible alternate number of strap-ons are shown for each maximum number in table 2.2. The six and eight strap-on designs offer the widest range of alternate configurations.

Another issue for each possible number of strap-ons is how the engines are allocated between the core and the strap-ons. Shown in table 2.3 are possible ways of placing the engines on the core and each strap-on so that there are 318 of them when all strap-ons are attached. One would like to match this engine allocation with the core/strap-on geometry, so that neither the core nor the strap-ons are carrying too many engines.

Geometrically speaking, the six strap-on configuration would consist of a core with six strap-ons that are of equal size to the core. Note that none of the ways of dividing the engines between the core and the strap-ons lead to an equal or near equal distribution of engines as shown in table 2.3. The eight strap-on case would have strap-ons that are smaller than the core, and the second choice of

Maximum Number of Strap-ons	Possible Engine Allocation	
	core	each strap-on
2	114	102
	126	96
4	66	66
	78	60
	102	54
6	30	48
	66	42
	102	36
8	30	36
	78	30
9	48	30
	102	24

Table 2.3: Possible division of engines between core and strap-on.

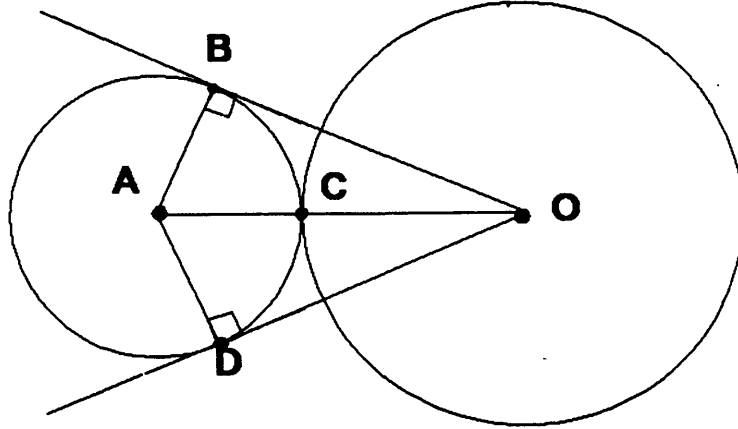


Figure 2.3: One of eight strap-ons attached to the core.

engine placement matches this. Thus, the eight strap-on configuration offers the advantages of many alternate configurations and straightforward engine placement; this will be the baseline.

Figure 2.3 shows the strap-on-core geometry. Let O be the center of the core, A the center of the strap-on, C the point of tangency, and points B and D the points of tangency of two lines drawn from the center of the core. For eight strap-ons, $\angle BOD$ is 45° , and $\angle BOA$ and $\angle DOA$ are each 22.5° . Thus,

$$\frac{BA}{AO} = \sin 22.5^\circ = 0.3826$$

Note further that $CA = BA$, since both are radii of the strap-on. This gives

$$\frac{CA}{CA + OC} = 0.3826$$

which, when solved, leads to

$$\frac{CA}{OC} = 0.6199 \tag{2.15}$$

In other words, the strap-on is 0.6199 or the diameter of the core, or 0.3843 of the area. Note how closely this area ratio matches the second engine placement scheme found above, where the ratio of strap-on to core engines is $30/78$ or 0.3846. This is desirable, because one must place a very large number of engines at the

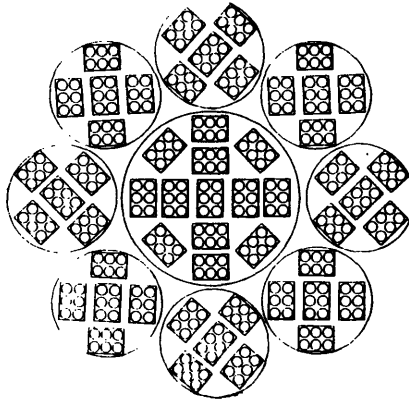


Figure 2.4: **A possible scheme for mounting the engines. Each strap-on has 30 engines, and the core has 78. The exact diameter of the core and strap-ons are determined later.**

bottom of each module, and it is better to spread the engines out as close to ideal as possible. Any other configuration would lead to too many core or too many strap-on engines. Thus, this initial design will have 30 engines on each strap-on and 78 engines on the core. This leads to the engine placement as shown in figure 2.4.

Given the cross-section geometry, the next issue is height. The two most apparent ways to scale the booster are as follows:

Option 1 *The boosters have the same height as the core. Their volume, and thus their mass, scale as the area, so each strap-on has a volume that is 0.3843 of the core volume.*

Option 2 *The boosters have the same ratio of height to width as the core. Their volume and mass scale as the area to the 3/2 power, so each strap-on has a volume that is 0.2382 of the core volume.*

The advantage of the first option is that each module has the same thrust to weight ratio, which means that the alternate configurations will have good performance. The advantage of the second scheme is that the fuel tanks in the core will have the same geometry as those of the strap-ons, leading to the same overall structural efficiency. To clarify the difference between these two options, consider a

	Option 1	Option 2
Core propellant	1,504,270 lbs	2,109,380 lbs
Core structure	167,140 lbs	234,380 lbs
Strap-on propellant	578,090 lbs	502,450 lbs
Strap-on structure	64,230 lbs	55,380 lbs
Liftoff Weight (2 strap-ons)	2,956,010 lbs	3,460,320 lbs

Table 2.4: **Liftoff weight comparison of strap-on height options.**

launch of a two strap-on alternate configuration. Given the volume ratios and the overall propellant mass, one can allocate m_{prop} between the core and the strap-ons. Given ε , one can then solve for m_{struc} , as

$$m_{struc} = \frac{m_{prop}\varepsilon}{1 - \varepsilon}$$

These lead to the results of table 2.4, neglecting the payload weight. The huge core of option 2 is a large burden when fewer than the maximum number of strap-ons is used, leading to the selection of option 1 as the initial baseline.

2.4.3 Propellant Tanks

Launch vehicles have been described as ‘flying gas tanks’ and from the numbers above, it is not difficult to see why. The primary structural element of launch vehicles is the tankage.

The propellant for this launch vehicle consists of liquid hydrogen and liquid oxygen. Hydrogen boils at -252.9° C (20° K) and has a density of 4.42 lb/ft³ (70.8 kg/m³). Oxygen boils at -183.0° C (90° K) and has a density of 71.2 lb/ft³ (1140 kg/m³). The conditions in the tanks will almost certainly be near boiling and this, combined with the need to force out large amounts of propellant, means that these tanks are also pressure vessels. This is one of the main reasons why propellant tanks

tend to have hemispherical or ellipsoidal end caps.

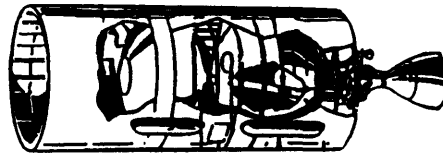
Figure 2.5 shows several existing tank configurations. [6, page I-3] [7, page 1-2] [8, fig. 1.6] In all cases, the tanks show the rounded end caps. Note that most of these tanks are 'long and skinny'; that is, they have round caps with long cylindrical barrel sections. In almost all of these cases, only a few engines had to be placed at the base of the vehicle and so, given transportation restrictions, the vehicles tend to be narrow. An exception is the integral tank shown on the Ariane. In this case, the smaller tank is made with a common bulkhead to the larger tank. The disadvantages of such a configuration is that it complicates the propellant feed and requires extensive insulation between the hydrogen and oxygen [8, page A1.13].

The RL10J uses a mixture ratio of 6:1, oxygen to hydrogen. This partially offsets the density difference shown above, and the hydrogen tank will be 2.68 times the volume of the oxygen tank. Thus, the hydrogen tank will consist of end caps and a barrel, and the diameter of the barrel will be sized by the oxygen tank. If the hydrogen tank is narrow enough, the oxygen tank will also be a capped cylinder. If the hydrogen tank is too wide, one will have an integral tank and/or a tank configuration that necks down. Figure 2.6 shows the three basic possibilities. One has to place 30 or 78 engines at the base of the stage, so the tank configuration must be of the second or third type, because these are wider than the first. Of course, the strap-ons and core do not have to have the same configuration. As a first try, the strap-on will use the second configuration, and the core will use either the second or third as necessary.

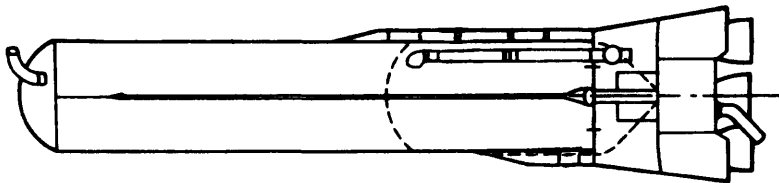
The strap-on contains 578,090 lbs of propellant. This corresponds to 495,510 lbs of liquid oxygen, or 6963 ft³. Assume that the tank consists of two ellipsoidal caps welded together. Figure 2.7 shows the geometry. An ellipsoidal pressure vessel cannot have a ratio b/a of less than $\sqrt{2}/2$, or the structure will experience compression near its equator, leading to buckling [9, page 28]. Assume that b/a is 0.75, like the



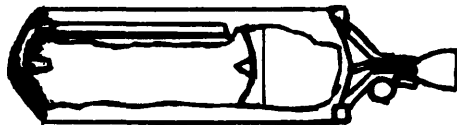
Titan III
First Stage
(N_2O_4 / Aerozine)



Titan III
Second Stage
(N_2O_4 / Aerozine)



Atlas
First Stage
(Liquid Oxygen/RP-1)



Ariane IV
Third Stage
(Liquid Oxygen/Liquid Hydrogen)

Figure 2.5: Several stages for several launch vehicles.

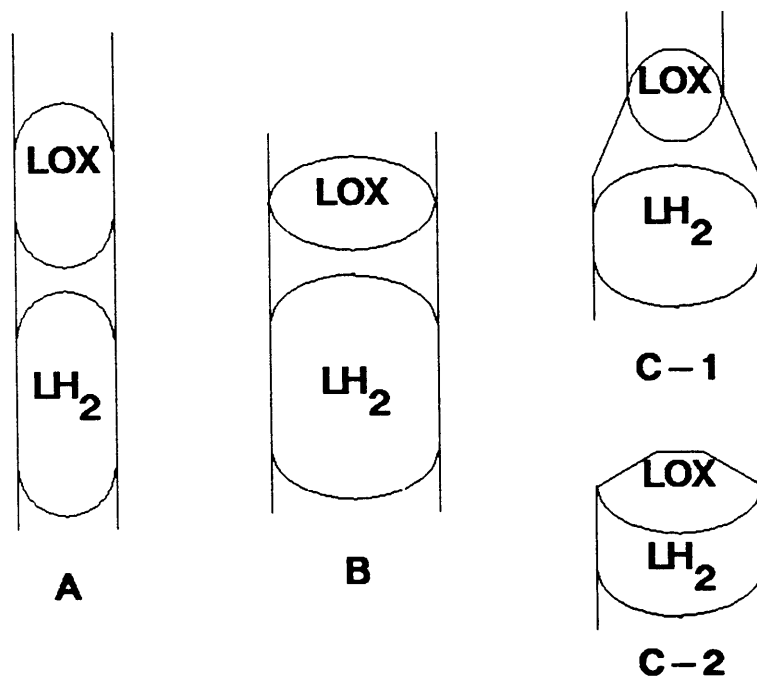


Figure 2.6: Three possible tank configurations. The first is similar to a Delta first stage; the second is similar to the Shuttle external tank; and the third (C-2) is similar to the Saturn S-IVB stage.

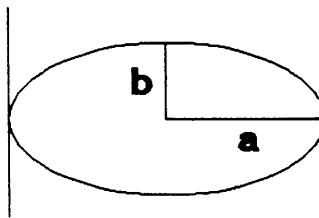


Figure 2.7: Cross section of an ellipsoidal tank. a is the semimajor axis, and b is the semiminor axis.

space shuttle external tank. This leads to

$$\frac{4}{3}\pi \cdot 0.75r^3 = 6963 \quad (2.16)$$

$$r = 13.04 \text{ ft}$$

and the strap-on will have a diameter of 26.1 ft (7.96 m).³

The simplest design for the hydrogen tank is to use the two parts of the oxygen tank as the end caps for the hydrogen tank. The only question is the height of the cylindrical barrel section. The end caps hold 6963 ft³, and there are 82,584 lbs (or 18,684 ft³) of hydrogen. Given the radius of 13.04 ft, this means that the barrel will be 21.94 ft (6.69 m) tall.

The next task is to size the core tanks. The core has 1,504,270 lbs of propellant, including 1,289,370 lbs of oxygen (18,116 ft³) and 214,900 lbs of hydrogen (48,619 ft³). Geometrically, equation 2.15 shows that the core is at least 42.1 ft in diameter. An ellipsoidal oxygen tank with b/a of 0.707 and radius 21.1 ft would have a volume of 27,618 ft³, which is about 50% too much. Thus, the core will have to use an integral tank or neck down to a spherical tank. Given the problems with integral tanks, a spherical oxygen tank will be used. The volume required leads to a spherical tank diameter of 32.6 ft (9.94 m).

The hydrogen tank can use ellipsoidal end caps. Using the ellipsoid calculated above, one will need to store 21,001 ft³ in the barrel section. This, combined with the 42.1 ft. diameter, leads to a barrel height of 15.09 ft (4.60 m). Overall, the strap on and core are as shown in figure 2.8. Also shown is an external view that gives an idea of the overall appearance of the launch vehicle.

³The shuttle external tank has a diameter of 27.5 ft, which is only a little too wide. Since this launch vehicle would probably require new tooling anyway, the 26.1 ft. diameter will be retained.

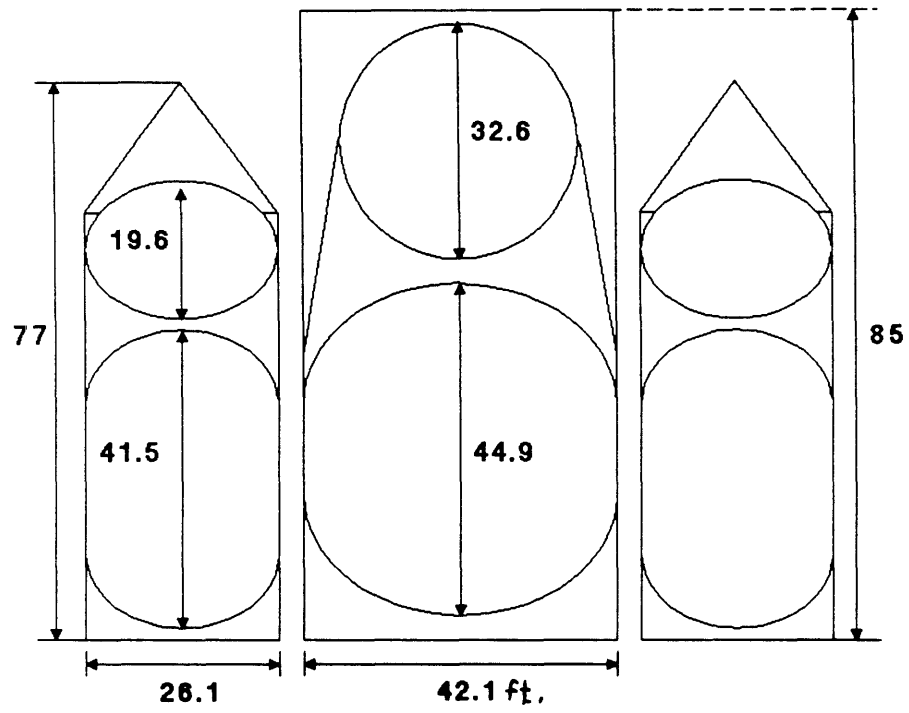


Figure 2.8: Cross section of core and strap-on.

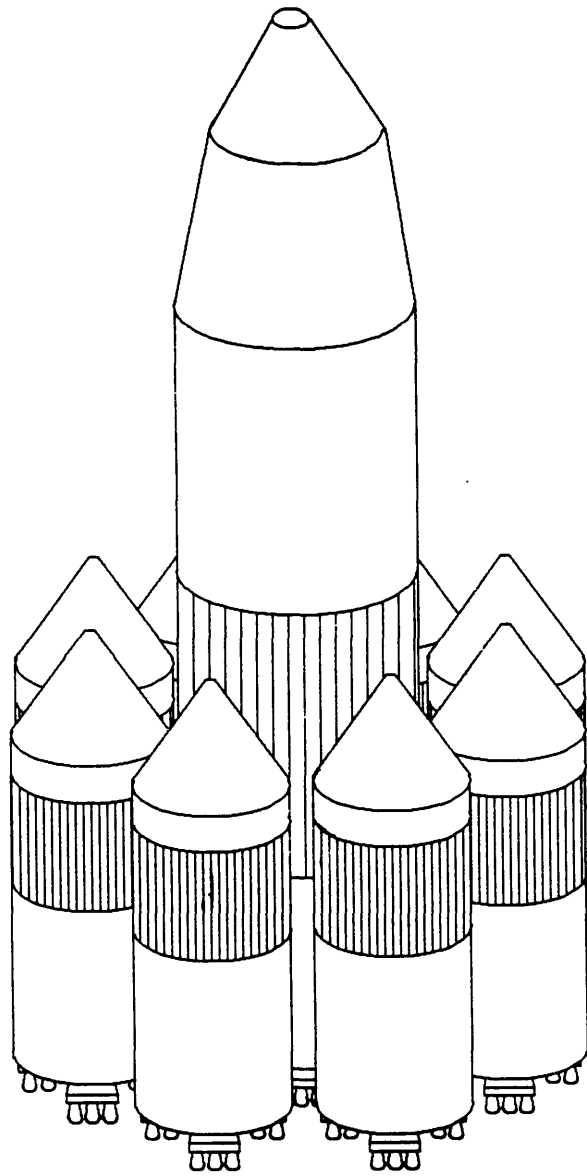


Figure 2.9: An external view of the launch vehicle as a whole.

Chapter 3

Performance Analysis

Given a design, the performance of the launch vehicle can be analyzed in detail. This analysis can be used to improve the design, validate the desired performance, and identify key operational characteristics of this type of launch vehicle. The performance analysis, in turn, requires an accurate simulator and certain assumptions about launch vehicle parameters.

3.1 Performance Analysis Background

3.1.1 The Trajectory Simulator

The performance and the trajectory of the launch vehicle were simulated using a program called PRO-Launch. This program integrates from flight event to flight event using a fourth-order Runge-Kutta integrator with fifth-order step size control. The program takes account of drag with lookup tables of C_D vs. Mach Number, and uses the 1976 U.S. Standard Atmosphere (with no winds) to find atmospheric properties. The only major flight parameter that is not taken into account is lift, but given small angles of attack and the fact that the drag (which is taken into account) will be much larger than any lift, this does not represent much loss in simulation accuracy.

Given a flight simulation, the vehicle must place its payload into a circular orbit at the desired altitude. The following scheme is employed as a simplified approach to guidance. The pitch angle at three specific times in the flight is variable. A constant pitch rate is selected between these angles such that the pitch angle is a continuous function of time. The program iterates on these three angles until the payload has been placed into a circular orbit of arbitrary altitude. The only other degree of freedom is the payload mass, and this is adjusted until the payload has been placed in the desired circular orbit.

The simulator is completely accurate as far as the integration is concerned, but its pitch profiles are empirically derived. In other words, the program is *correct*, but it may not be *optimal*. This slight loss of optimality is offset by a tremendous gain in simplicity and ease of use, and this led to the selection of PRO-Launch as the simulator. Thus, each data point below represents a fully detailed simulation of the flight of the vehicle.

3.1.2 Vehicle Assumptions

There are many variables that go into a launch vehicle simulation. The following tables list all of the variables used to simulate the performance. (All of the inputs into the program are in metric units, so they are listed first.)

Masses:

Component	Mass	Weight
Core Inert Weight	75813.2 kg	167140 lbs
Fairing Weight	11340.0 kg	25000 lbs
Core Propellant Weight	682325.4 kg	1504270 lbs
Strap-on Inert Weight	29134.2 kg	64230 lbs
Strap-on Propellant Weight	262217.2 kg	578090 lbs

Source: Table 2.4; fairing weight based on Hughes design.

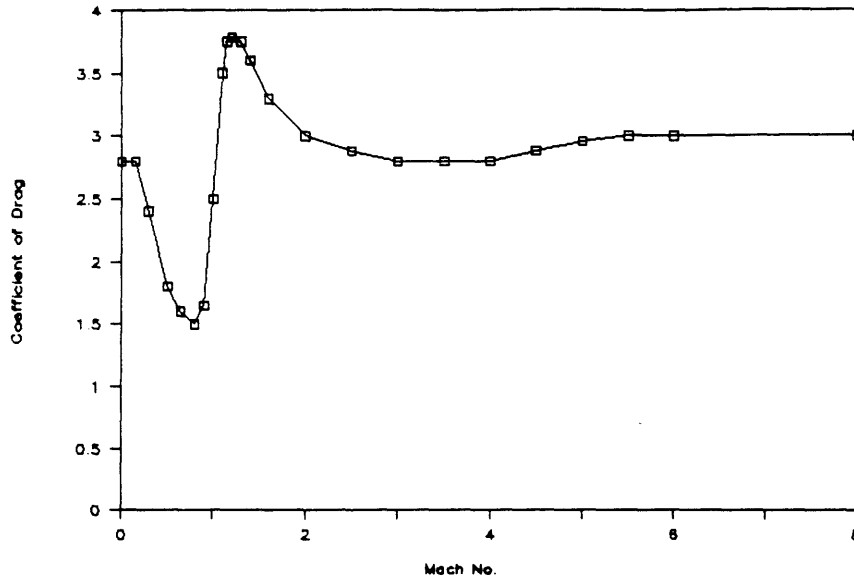


Figure 3.1: C_D plotted as a function of Mach Number.

Engines:

Parameter	Metric Unit	English Unit
Number	(30 per strap-on) (78 on core)	
I_{sp}	4050 N sec/kg	413 sec.
Vacuum Thrust	152026 N	34176.8 lbf
Nozzle Exit Area	0.3158 m ²	3.399 ft ²
Source	Pratt and Whitney	

The program uses a back pressure correction based on local atmospheric pressure to find the thrust while in the atmosphere.

Aerodynamics:

See figure 3.1 for a graph of the coefficient of drag as a function of the Mach Number. The reference area used is 71.181 m² (766 ft²). The C_D curve is the same as that being used for the Hughes design, and was obtained by the careful analysis of Dr. C. P. Liu of Hughes. A comparison of the shape of the Hughes design and this design is

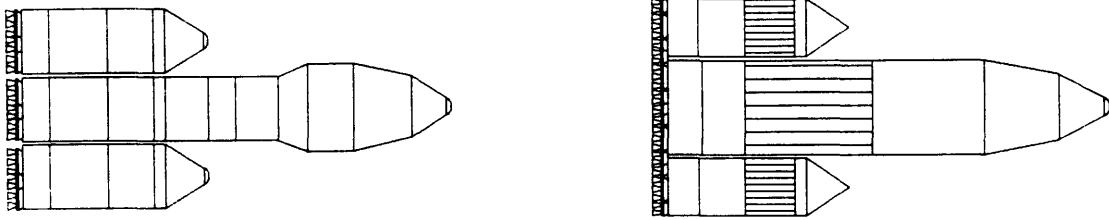


Figure 3.2: At left is a cross section of the Hughes design. At right is a cross section of this design.

shown in figure 3.2; the two are similar. The reference area used in this analysis is not the geometric area of the core or the strap-ons. It was calculated from the reference area used for the Hughes design and multiplied by the ratio of the total frontal areas of the two designs. This allowed for accurate calculation of drag without recalculating every point on the C_D curve.

Other parameter assumptions:

Target Orbit: 185.2 km perigee and apogee altitude
(100 naut. mi.)

28.5° inclination

Launch Site: 28.5°N, 80.6°W; (Kennedy Space Center)

5 m (16ft) altitude above sea level

Source: Section 2.1

G-limit: 3.0 g's acceleration

The last parameter is the upper limit on the perceived acceleration of the payload. When this limit value is reached, a certain number of engines are shut down. In these cases, 10% of the active engines are shut down when the g-limit is reached.

Mission sequence:

Time (sec.)	Event	Comments
0	Liftoff	Begin vertical ascent
30	Begin pitchover	Delay assures adequate thrust/weight ratio
86	Shut down core engines	Preserves propellant for use after strap-ons burn out.
195-240	g-limitation	Maximum acceleration limited by shutting down strap-on engines as necessary
235	8 core engines restarted; 1 engine per strap-on shut down	Assures positive g's after strap-on separation, eliminating the need for settling rockets
240	Strap-on burnout and separation	Separated for recovery
245	70 core engines restarted	Engines not started above are started now
330-410	g-limitation	Maximum acceleration limited by shutting down core engines as necessary
420	Burnout	Payload placed in orbit

The pitch angle iteration points are at 160, 290, and 420 seconds.

Source: events are from Hughes launch vehicle design; times are unique to this configuration. All but the first three times listed above vary from run to run depending on the exact configuration being simulated.

3.1.3 Analysis Methodology

The procedure for analyzing the payload capacity of this design is as follows. First, a series of optimizing trade studies will be carried out by varying vehicle parameters and selecting those values which maximize payload within constraints. These parameters include liftoff weight, core/strap-on size ratio, core/strap-on engine number ratio, g-limit, and core shutdown time. Note that each of these parameters can be chosen in advance by the designer. The end result of this phase will be an improved vehicle design.

Second, a series of analyses will be carried out which show how the performance changes when certain other parameters are varied. These other parameters cannot be chosen by the designer, but may turn out to have values higher or lower than expected. These parameters include mass fraction (ϵ), drag, number of strap-ons, and specific impulse (I_{sp}). The end result of this phase will be an understanding of how 'robust' the design is to changes in externally determined parameters.

This section concludes with a detailed trajectory presentation. (The output of PRO-Launch is in English units, and all of the results below are tabulated in English units.)

3.2 Trade Studies

3.2.1 Liftoff Weight

The first parameter that will be varied is the total liftoff weight. For this analysis, all of the system parameters listed above are held constant except for the masses. The core and strap-on propellant masses are increased while holding the ratio of core to strap-on propellant constant. The mass fraction of 0.1 is also held constant, so the increased propellant masses mean increased structural masses. The results of this study are presented in table 3.1 and graphed against the total weight in

Core Propellant Load (lbs)	Strap-on Propellant Load (lbs)	Total Takeoff Weight (klbs)	Payload to LEO (lbs)	Takeoff Thrust/Weight
1,504,000	578,000	7167	332,000	1.198
1,524,000	586,000	7252	334,900	1.184
1,558,000	599,000	7415	339,400	1.158
1,564,000	601,000	7447	339,300	1.153
1,584,000	609,000	7538	340,200	1.139

Table 3.1: **Results of variation in liftoff weight.**

figure 3.3. (LEO in all of the tables below is an abbreviation for low Earth orbit.)

The points on the graph do not lie on a straight line or simple curve. This is probably due to a certain margin of error in the results of the simulator. However, rather than calculating more data points, the overall trend is already apparent, and greater takeoff mass means more payload. Since this is a ‘trial and error’ optimization instead of a mathematical optimization, no greater accuracy is needed and this general result is sufficient.

Note that increasing liftoff weight means decreasing thrust/weight ratio at liftoff. Most boosters have a takeoff thrust/weight ratio of 1.3 to 2.0; a major drawback of this small engine design is a lower thrust/weight ratio than normal. This ratio is important if one is to clear the launch pad in a reasonable amount of time and build up enough speed to maintain control in the atmosphere. While the limit on this ratio seems to be a subjective matter, a reasonable lower limit seems to be a ratio of 1.1 with 5% of the engines out. This gives a minimum thrust/weight ratio of 1.158 at liftoff with all engines firing, and constrains one to select the third data point as the maximum liftoff weight.

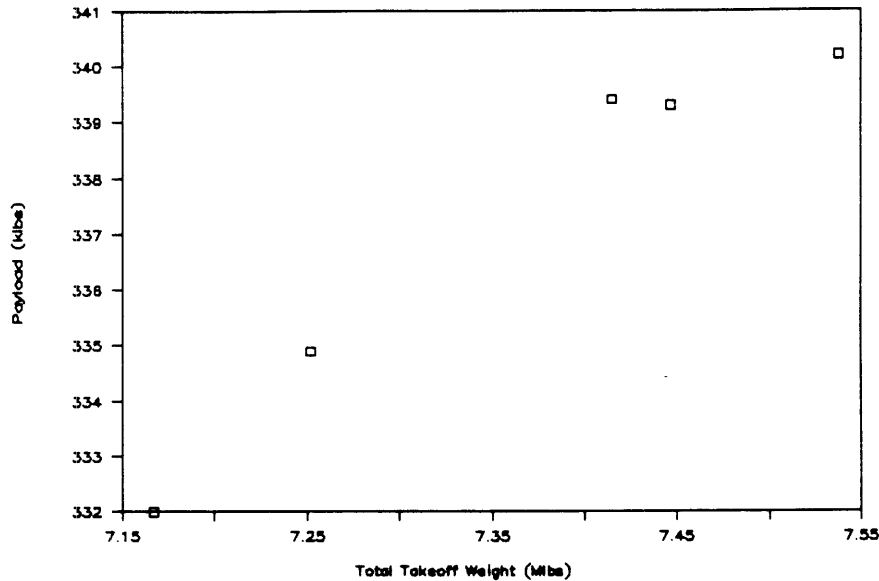


Figure 3.3: Payload as a function of liftoff weight.

3.2.2 Core/Strap-on Size Ratio

The next parameter to be varied is the ratio of the core size to strap-on size. As above, all of the parameters are held constant with the exception of the masses. This time, the total liftoff weight and the mass fractions are held constant while the ratio (core propellant/strap-on propellant) is increased. Holding liftoff weight constant predetermines the strap-on weight once a core weight is selected, and this weight is broken down into propellant and structure using the mass fraction. The result of this variation is presented in table 3.2.2 and in graphic form in figure 3.4.

Note that, in this case, there is a clear maximum in terms of performance. This leads to the selection of the third set of parameters as the new baseline with the added bonus that the strap-on size is essentially the same as was calculated above, eliminating the need for strap-on redesign.

The core, however, does need redesign. The new size gives more liquid oxygen and hydrogen than before. Assuming that the tanks are designed with the same geometry as above, the newer core would have a 34 ft (10.4 m) diameter sphere for the liquid oxygen and a 49.8 ft (15.2 m) tall liquid hydrogen tank with a 20.0 ft

Core Propellant Load (lbs)	Strap-on Propellant Load (lbs)	Core/Strap-on Size Ratio	Payload to LEO (lbs)
1,598,000	594,000	2.69	340,200
1,678,000	584,000	2.87	341,100
1,718,000	579,000	2.97	341,100
1,758,000	573,000	3.07	340,900
1,838,000	564,000	3.26	338,900

Table 3.2: Results of varying core/strap-on size ratio.

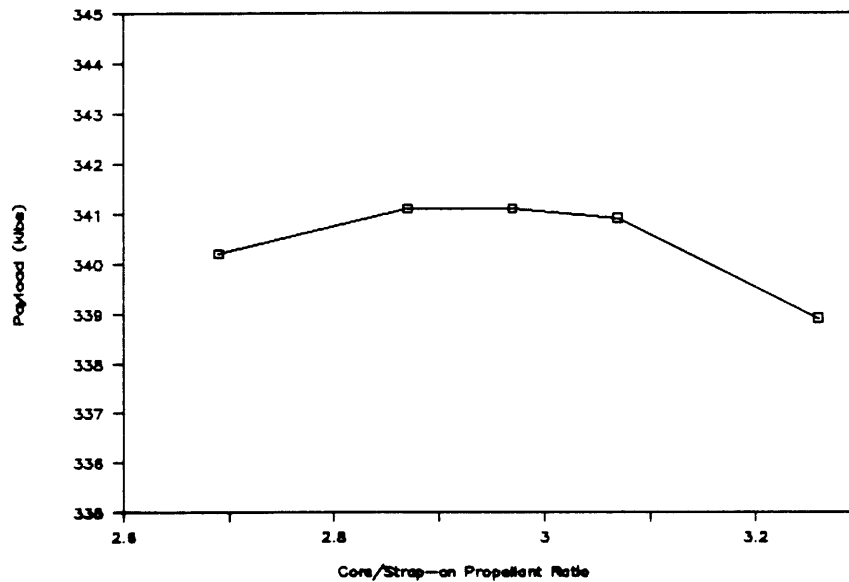


Figure 3.4: Payload to LEO as a function of the ratio of core to strap-on size.

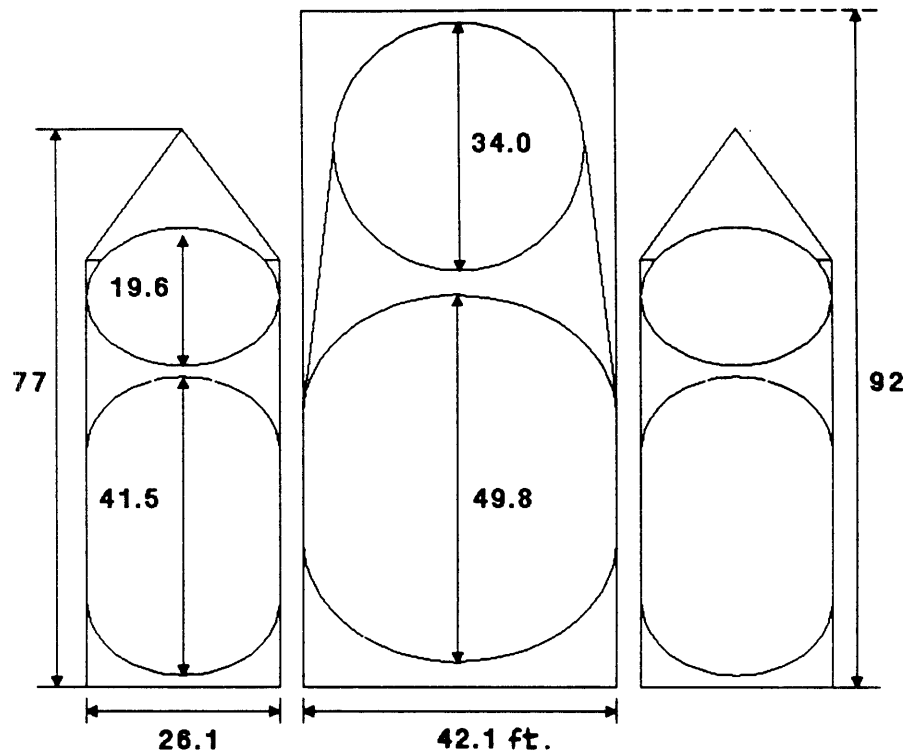


Figure 3.5: Launch vehicle cross section with improved tank sizing.

(6.10 m) barrel section. This newer design is shown in cross section in figure 3.5. This will be the final sizing of the propellant tanks.

3.2.3 Core/Strap-on Engine Ratio

The next analysis will be to determine whether the 30/78 engine placement scheme is the best arrangement. To carry this out, the total number of engines is kept at 318, while the breakdown of this total between core and strap-ons is changed, neglecting the fact that this results in numbers of engines that would be difficult to cluster. All other vehicle parameters are kept constant. The results are presented in table 3.3 and in figure 3.6.

This analysis shows that one would prefer to have as many engines as possible on the strap-on, which leads to the question of the maximum number of engines that can be placed on each strap-on. Shown in figure 3.7 are the current engine

Number of Engines		Payload to LEO (lbs)
Strap-on	Core	
32	62	351,000
30	78	341,100
28	94	322,300

Table 3.3: Results of alternate engine placement.

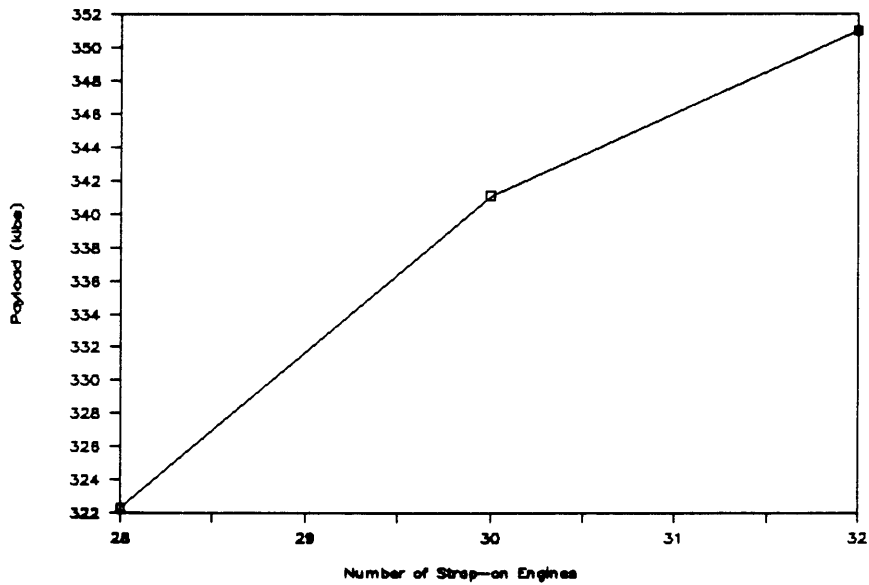


Figure 3.6: Payload plotted as a function of the number of strap-on engines. (The number of core engines is such that the total number of engines remains at 318.)

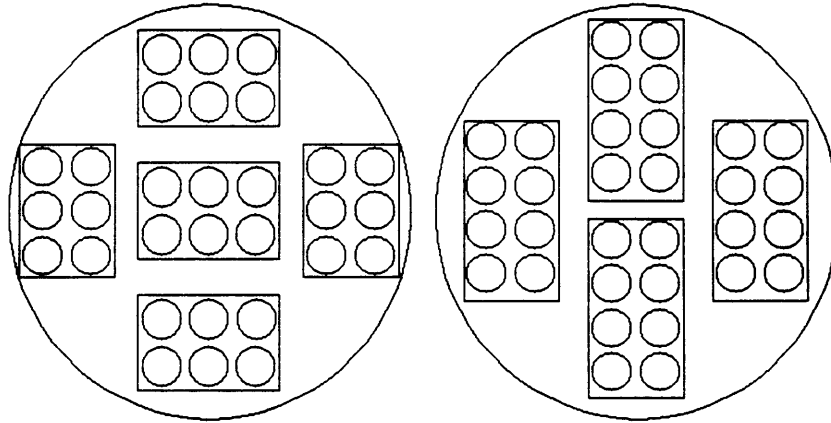


Figure 3.7: **Two engine placement schemes.**

placement scheme and an alternative for 32 engines. As seen, the alternate scheme does not offer the same control authority as the basic design; the engines do not have room to gimbal about two axes. Because of this, the engine scheme will be kept as it is. ¹

3.2.4 Acceleration Limit

As mentioned above, the vehicle turns off a suitable number of engines when the perceived acceleration reaches a preset g-limit. To find the best limit, this g-limit is varied, and the level to which the vehicle is ‘throttled’ is kept at 90% of the g-limit. (For example, if the vehicle has a 4.0 g limit and reaches this level, enough engines are shut down to bring the acceleration down to 3.6 g’s.) All other vehicle parameters are kept constant. The results are presented in table 3.4 and in figure 3.8. (The 2.0 g limit represents a special case. The core shutdown time of 86 seconds

¹One could use thrust vector control by injection instead of gimbaling. Gimbaling is better defined and understood, so it will be retained; a growth version of this vehicle could use injection and so have more engines. Injection is further discussed in section 4.3.3.

G-Limit	Payload to LEO (lbs)
2.0	326,300
2.5	340,400
3.0	341,100
3.5	340,600
4.0	340,400

Table 3.4: Results of varying acceleration limit

was changed to a core shutdown zone from 85 to 125 seconds.)

The only reason that this scheme is feasible is the very large number of engines present. The number allows the total thrust of the vehicle to be controlled with precision, but does not require throttling of individual engines. The engines are simply turned on or off as needed, eliminating the need for possibly expensive throttling provisions.

The result of this analysis is that there is no gain in payload with a limit above 3.0 g's. The reason for this is as follows: the only effect that a higher g-limit has is that it shortens the burn time and thus lowers the gravity loss. As seen from the sample mission sequence above, the choice of g-limiting scheme only begins to make a difference in trajectory after about 195 seconds. But, by 195 seconds into the flight, the vehicle has already pitched over to a low angle. The geometry of the acceleration on the vehicle has become similar to that of a spacecraft in orbit, and the further effect of gravity on actual ΔV is minimal. (The software simulation makes use of an accurate central acceleration model instead of a 'flat Earth.')

Thus, choice of g-limit has at most a second order effect above a certain threshold. The limit of 3.0 g's is retained as it provides relief for satellite designers while maintaining a comfortable margin over the threshold. This is a key advantage of this design, as

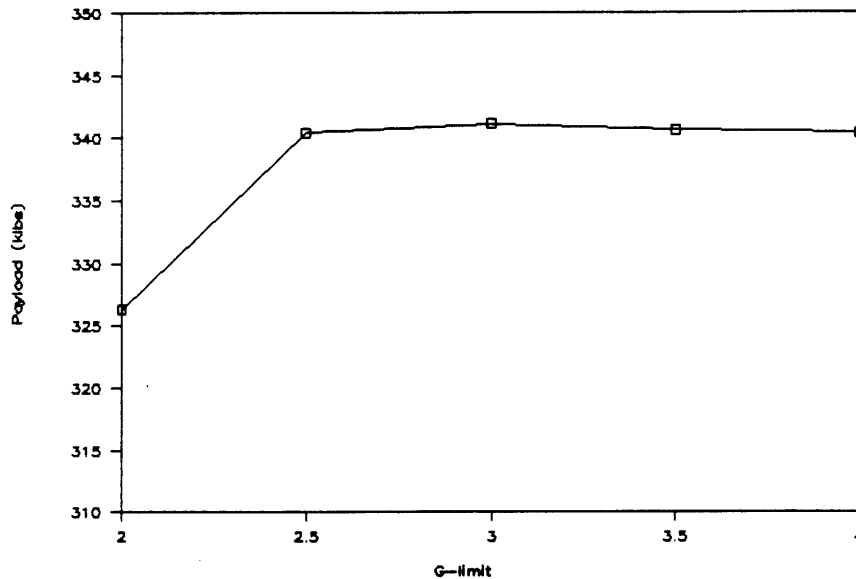


Figure 3.8: **Payload as a function of the upper acceleration limit**

it allows the customer to determine how soft the ride will be. If one is willing to accept a loss in payload capability, the acceleration can be limited to as low as 2.0 g's.

3.2.5 Core Shutdown Time

The next area of analysis is that seemingly arbitrary core shutdown time of 86 seconds. To carry this out, all of the vehicle parameters are held constant while the core shutdown time is varied up and down. The result is presented in table 3.5 and in figure 3.9.

As seen, the general trend is that an earlier core shutdown time means more payload. However, there is another constraint. About 80 seconds into the flight, the vehicle passes through maximum dynamic pressure, the time when the aerodynamic stresses on the structure of the vehicle are most severe. One wants to minimize the time spent flying through this flight regime as much as possible, so one wants to leave all of the engines on until at least 80 seconds into the flight. To provide a comfortable margin, this time will be kept at 86 seconds.

Core Shutdown Time (sec.)	Payload to LEO (lbs)
70	343,500
80	341,300
86	341,800
90	339,700
100	336,200

Table 3.5: Results of varying core shutdown time.

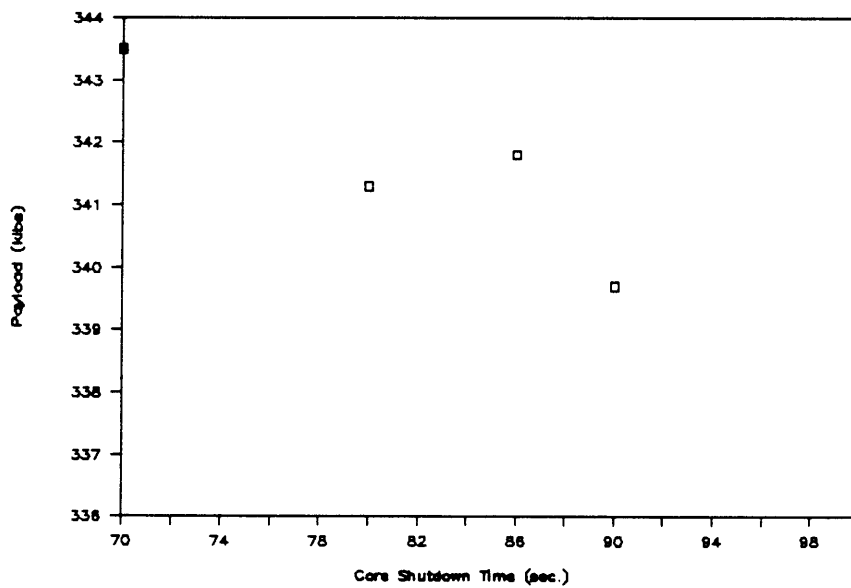


Figure 3.9: Payload as a function of the core shutdown time.

3.2.6 Trade Study Summary

The trade studies above have all maximized the payload capacity within certain constraints. The fuel loading in the core and strap-on provides for maximum payload delivery, subject to a liftoff weight constraint. The engine placement must remain the same to provide enough room for gimbaling. Acceleration limits have almost no effect on payload above a certain threshold, and so the previous limit is retained. The core shutdown time remains the same because of aerodynamic constraints. The result of this phase of analysis is a vehicle size, engine placement scheme, and mission sequence that can deliver the maximum payload subject to several constraints.

3.3 Variation Studies

3.3.1 Mass Fraction

The first parameter that will be varied is the mass fraction. As mentioned in the derivation, a mass fraction of 0.1 seems reasonable, but after design and construction this figure could move up or down. For the following analysis, all of the vehicle parameters are held constant except for the inert stage weights. In other words, the propellant weights are held constant while the stage weights change, resulting in a change in mass fraction. The mass fraction of the core and strap-ons are varied separately.

Core Mass Fraction

Since the core goes to orbit along with the payload, the gain or loss in core mass is precisely equal and opposite to the loss or gain of payload mass. (This analysis is the only one which does not use computer simulation for each data point as the one-to-one relation makes the payload variation a straightforward calculation.) This

Core Mass Fraction	Core Inert Weight (lbs)	Payload to LEO (lbs)
0.11	212,300	319,900
0.10	190,900	341,800
0.09	169,900	362,300

$\frac{\partial \text{payload}}{\partial \text{core weight}}$ is 1.0 lb/lb, and $\frac{\partial \text{payload}}{\partial \text{core mass fraction}}$ is 21200 lb/percentage point.

Table 3.6: Results of varying core inert weight.

leads to the results presented in table 3.6. (The nominal values are in boldface in this and all subsequent tables.)

Strap-on Mass Fraction

To carry out this variation study, the core weight is held constant while the strap-on inert weight is varied. The results are presented in table 3.7 and in figure 3.10.

The effects of the variation in strap-on and core inert weights add, so an addition of 1.0 lb to each strap-on *and* the core would result in a 3.0 lb loss of payload.

3.3.2 Drag

As mentioned above, the profile of drag coefficient versus Mach number was based on a slightly different geometry than that of this launch vehicle. To study the effect of inaccuracies in drag on payload, the drag is multiplied by a constant ranging from 0.5 to 2.0. (In software, this is accomplished by changing the reference area, the simplest way to assure constant variation at all points.) All other parameters are held constant at their nominal values. This variation results in the payload

Strap-on Inert Weight (lbs)	Strap-on Mass Fraction	Payload to LEO(lbs)
54,300	0.086	361,600
59,300	0.093	351,600
64,300	0.100	341,800
69,300	0.107	331,400
74,300	0.114	321,400

$\frac{\partial \text{payload}}{\partial (\text{inert weight of each strap-on})}$ is 2.0 lb/lb, so $\frac{\partial \text{payload}}{\partial (\text{total strap-on inert weight})}$ is 0.25 lb/lb.
 $\frac{\partial \text{payload}}{\partial (\text{mass fraction of each strap-on})}$ is 14400 lb/percentage point.

Table 3.7: Results of varying strap-on inert weight.

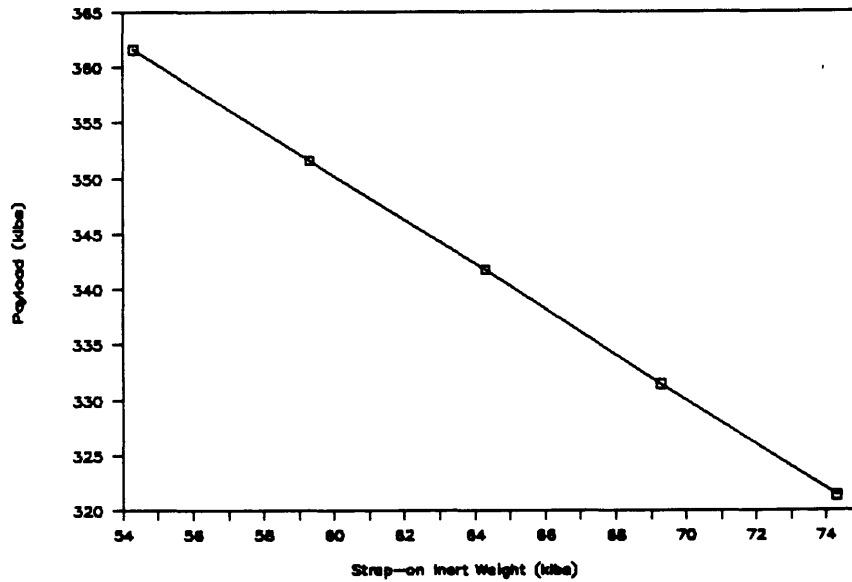


Figure 3.10: Payload variation as a function of variation in strap-on inert weight.

Drag Factor	Payload to LEO (lbs)
0.5	357,800
1.0	342,800
1.5	326,900
2.0	312,600

$\frac{\partial \text{payload}}{\partial \text{drag factor}}$ is 300 lb/percentage point.

Table 3.8: Results of varying drag.

variation shown in table 3.8 and graphed in figure 3.11.²

The change is small: a drag multiplier of 2.0 results in a 10% decrease in payload. This can be seen from first principles, as ΔV_D is only a small fraction of ΔV_{∞} .

3.3.3 Number of Strap-ons

When there is less than 343,000 lbs of payload to launch, one can use fewer than eight strap-ons. The payload capacity of the three alternate configurations is presented in table 3.9 and in figure 3.12. The two strap-on configuration uses an initial 25% offload in the strap-on propellant to improve performance, and all other vehicle parameters are kept at their nominal values.

The results show a great range of payload capability using the same system, highlighting a benefit of modularity. However, it is doubtful that the capability shown at the ‘small end’ is competitive. The Titan IV launch vehicle has about the same capability to LEO, but is all expendable. The configuration shown above would require recovery of two strap-ons and expend a core with 78 engines on it. A detailed cost analysis would be needed to determine which is actually cheaper.

²The slight change in nominal payload is a result of correcting a small error in the atmosphere model.

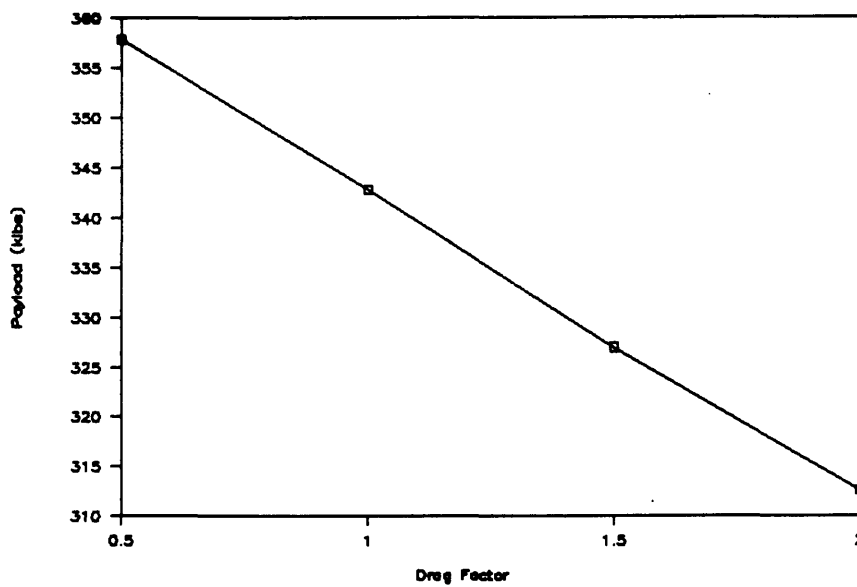


Figure 3.11: Payload variation due to variation in drag. The nominal drag is multiplied by the constant shown.

Number of Strap-ons	Payload to LEO (lbs)
2	43,000
4	157,000
6	254,400
8	342,800

Table 3.9: Results of varying the number of strap-ons.

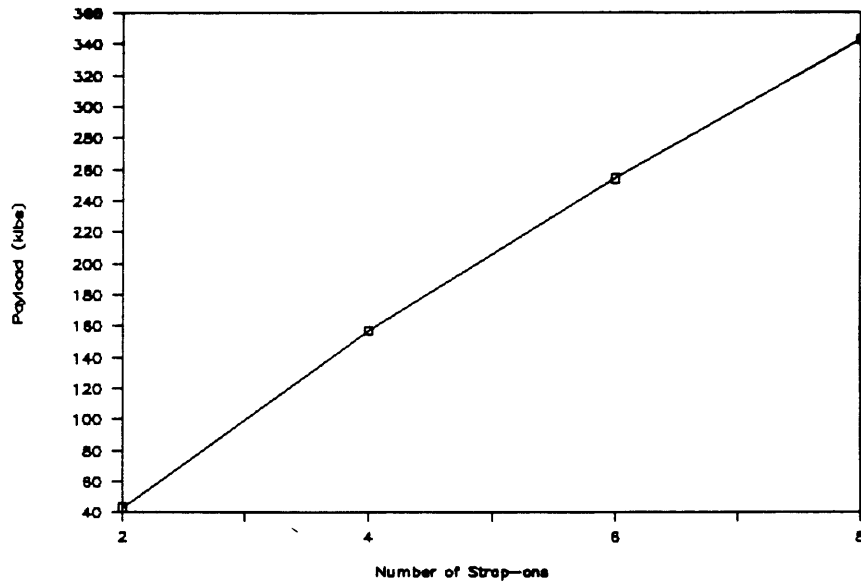


Figure 3.12: Payload carried by alternate configurations.

3.3.4 Specific Impulse

The vacuum specific impulse (I_{sp}) of the RL10J is 413 seconds. If these engines are not available, or if one wants to modify the RL10J to a higher or lower I_{sp} , one needs to know what effect it will have on payload. For this analysis, the mass flow rate (\dot{m}) is held constant (82.8 lbm/sec, or 37.5 kg/sec). Since $T = \dot{m}gI_{sp}$, the thrust of the engines increases or decreases with I_{sp} . The results are presented in table 3.10 and graphed in figure 3.13. Noting the scale of the graph, the payload is quite sensitive to changes in I_{sp} .

3.3.5 Variation Study Summary

The final mass fraction and I_{sp} of the vehicle will have a fairly large impact on the payload capacity. Of the parameters varied in the trade and variation studies, these two showed the largest change in payload to orbit. Thus, if this vehicle, or any one like it, is ever built, steps would have to be taken to assure that these two parameters are accurately determined and maintained. Quite the opposite is true of drag; since major changes in drag result in minor changes in payload, any reasonable

Vacuum I_{sp} (sec.)	Vacuum Thrust (lbf)	Sea Level Thrust (lbf)	Payload to LEO (lbm)
403	33,300	26,200	298,100
408	33,800	26,600	320,100
413	34,200	27,000	342,800
423	35,000	27,800	387,300

$\left(\frac{\partial \text{payload}}{\partial \text{vacuum } I_{sp}}\right)_m$ is 4460 lb/sec.

Table 3.10: Results of varying the specific impulse.

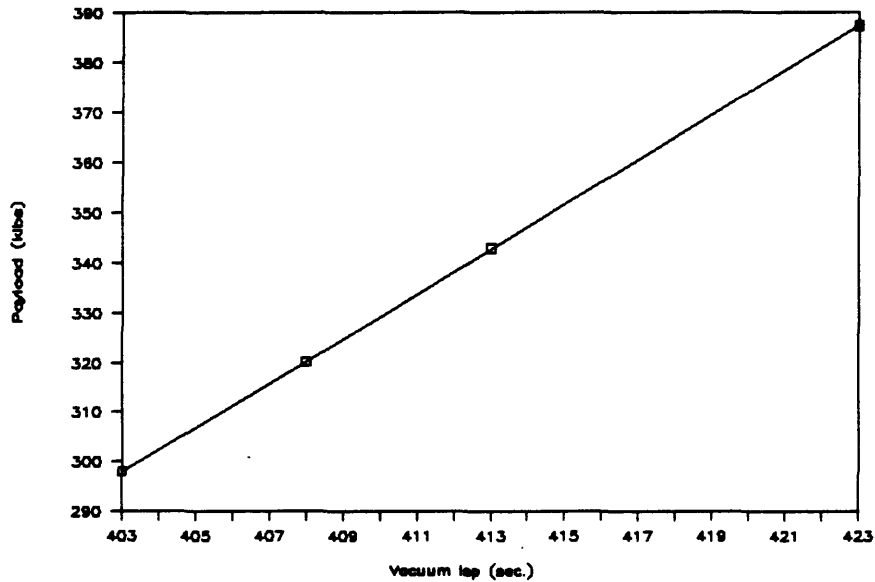


Figure 3.13: Payload variation with a variation in the specific impulse of the engines.

estimate of drag should result in a good estimate of payload. The payload carried by alternate configurations shows the flexibility of this highly modular design.

3.4 Trajectory Description

Below is a series of graphs that depict many key trajectory parameters as functions of time. Many of these parameters show the same profile as with any launch vehicle, but some show features unique to this design.

The first graph (figure 3.14) is one of downrange distance versus altitude. This gives one a physical feel for the shape of the trajectory as well as summarizing the time and location of major flight events.

The next three graphs are of altitude, *relative* velocity (or airspeed), and weight as functions of time (figures 3.15 through 3.17). All of these graphs are not all that different from existing launch vehicles. The dramatic effects are primarily due to mission sequence events; for example, the staging of the strap-ons show as a bend in the graph of weight versus time.

The next two graphs (figures 3.18 and 3.19) show the pitch and flight path angle as functions of time respectively. Pitch is defined as the angle between the *thrust* vector and the local horizontal, while flight path angle is defined as the angle between the *velocity* vector and the local horizontal. The pitch is less than zero at burnout because the vehicle must thrust downward in order to circularize. The graph shows the effect of the simplified guidance scheme discussed in section 3.1.1. The flight path angle reaches zero at burnout as the vehicle is going into a circular orbit.

The next two graphs (figures 3.20 and 3.21) show drag and dynamic pressure as respective functions of time. Both have a sharp peak as in the example used to estimate ΔV_D in advance (figure 2.2). The graphs of thrust and perceived acceleration (figures 3.22 and 3.23) show the result of g-limitation. The acceleration reaches

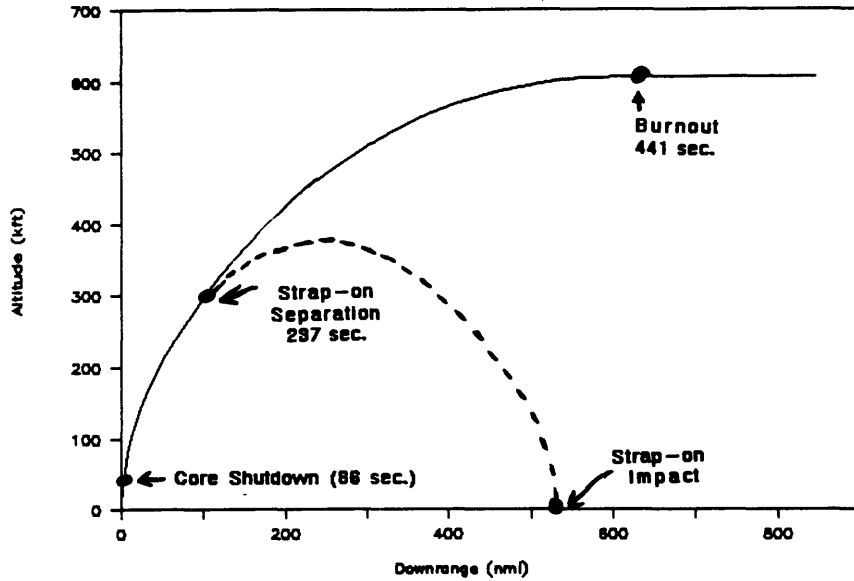


Figure 3.14: A side view of the trajectory with key event times and locations.

and stays within a 'deadband' between 2.7 and 3.0 g's. Numerical integration of the graph of acceleration yielded a true propulsive ΔV of 30,120 ft/sec (9180 m/sec). This shows that the initial estimate of 32,300 ft/sec (9850 m/sec) was very conservative and it explains why the payload capability is 42,800 lbs greater than that for which the vehicle was initially sized.

The last figure (3.24) is a map showing the vacuum instantaneous impact points. These points are the location where the launch vehicle would hit if the thrust went to zero at the stated time and if there was no atmosphere. This is important for range safety reasons; to put it bluntly, this map shows where the pieces would come down if the vehicle blows up at a certain time. Also shown on this map is the impact location of the strap-ons.

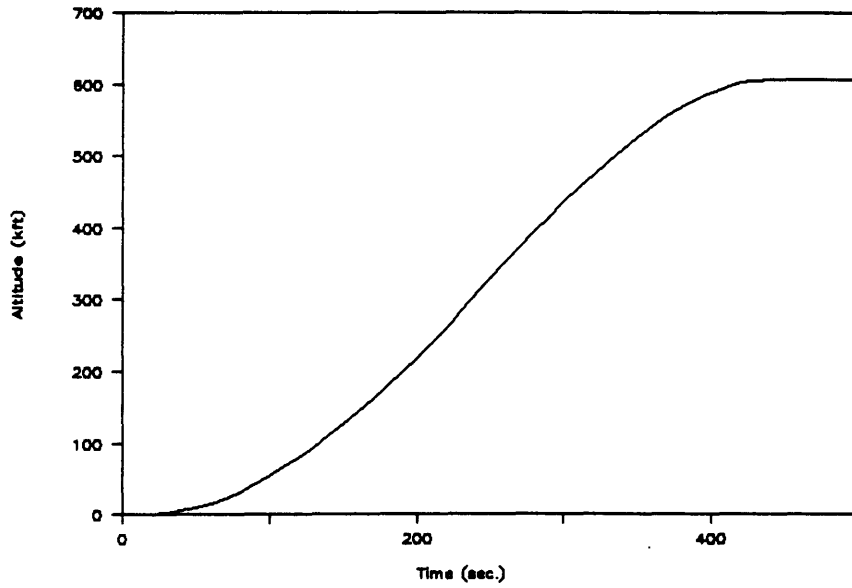


Figure 3.15: The altitude of the launch vehicle as a function of time.

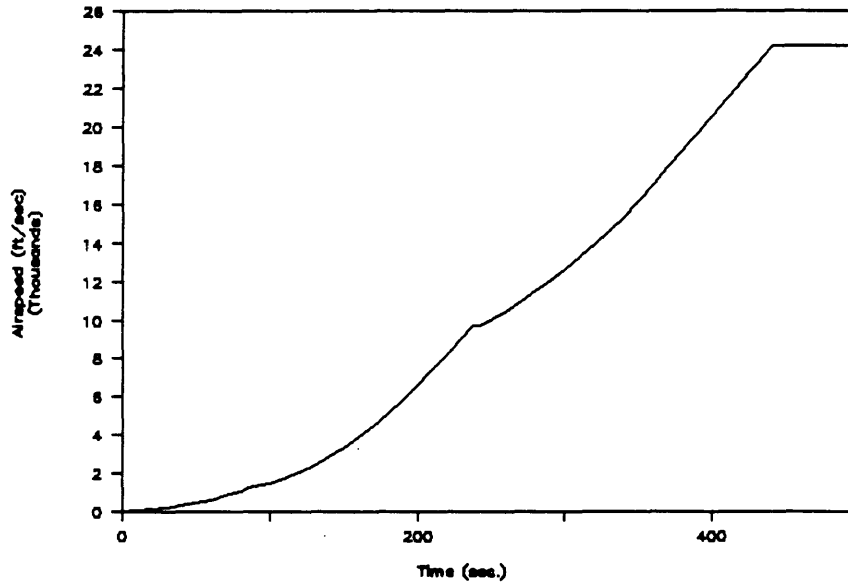


Figure 3.16: The airspeed of the launch vehicle as a function of time.

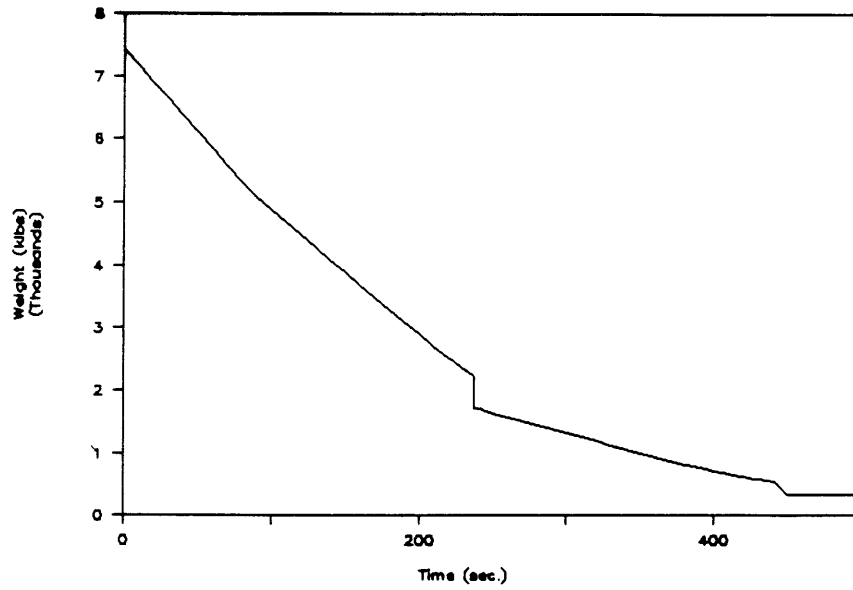


Figure 3.17: The total weight of the launch vehicle as a function of time.

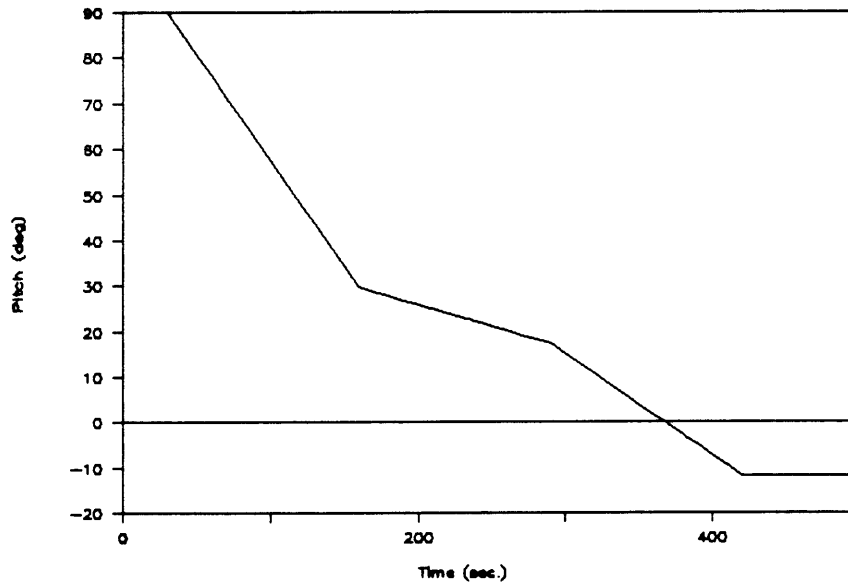


Figure 3.18: The pitch of the launch vehicle as a function of time.

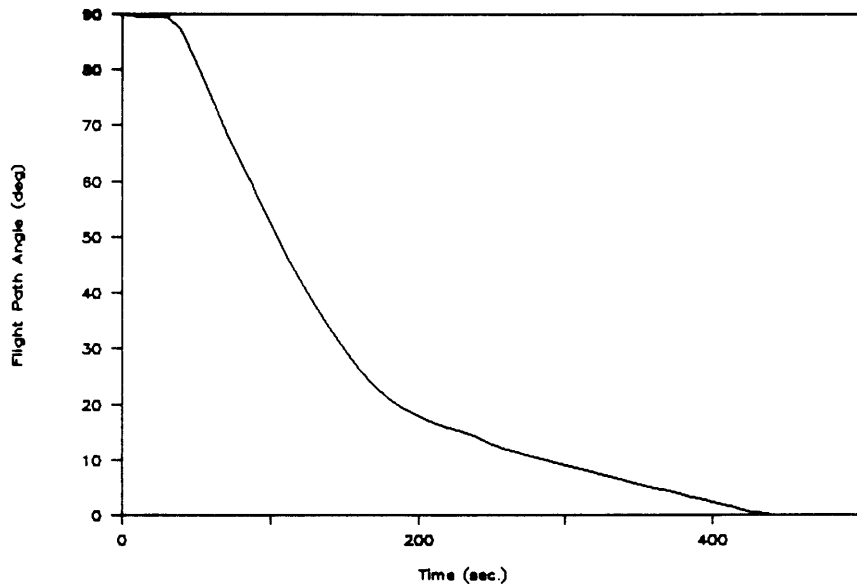


Figure 3.19: The flight path angle of the launch vehicle as a function of time.

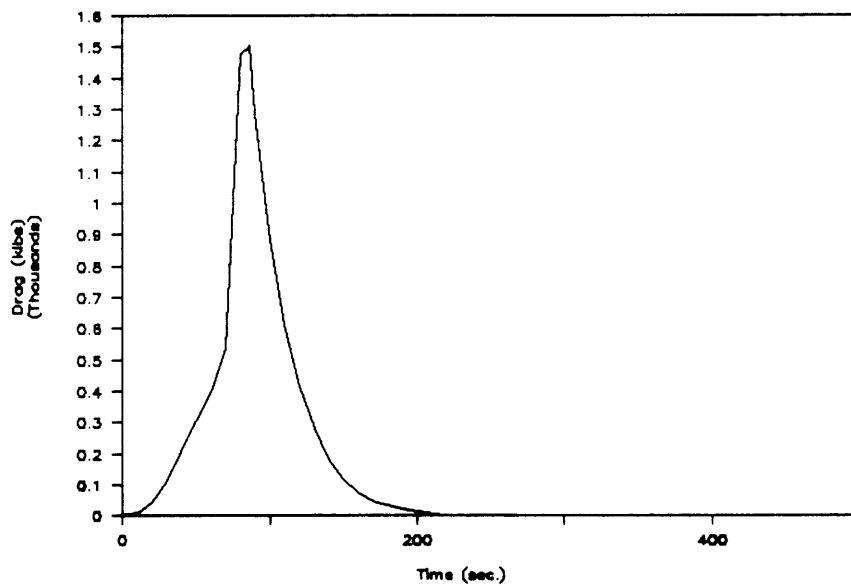


Figure 3.20: The drag of the launch vehicle as a function of time.

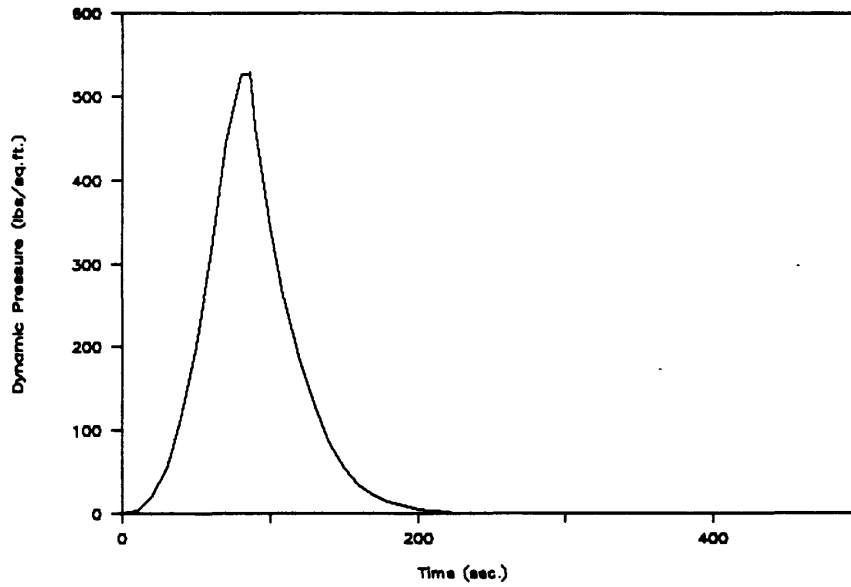


Figure 3.21: The dynamic pressure on the launch vehicle as a function of time.

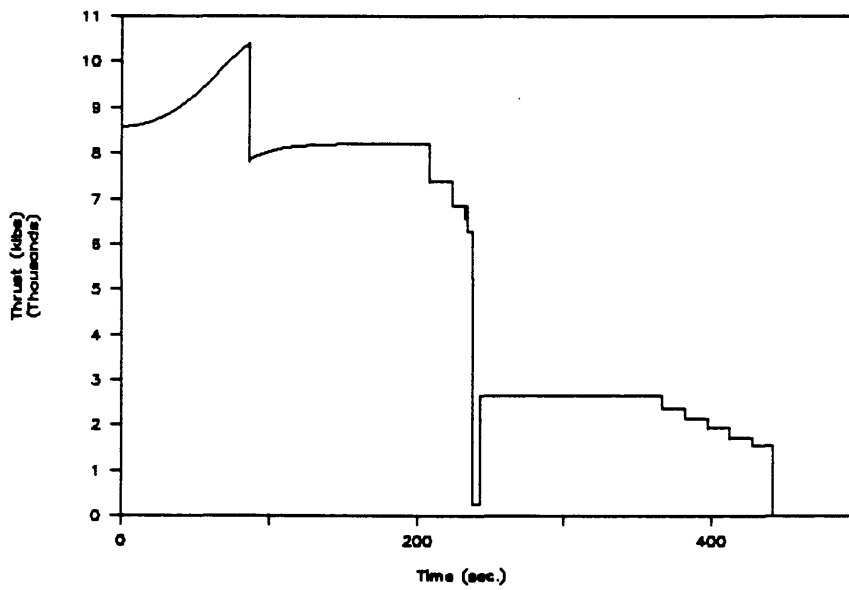


Figure 3.22: The thrust of the launch vehicle as a function of time.

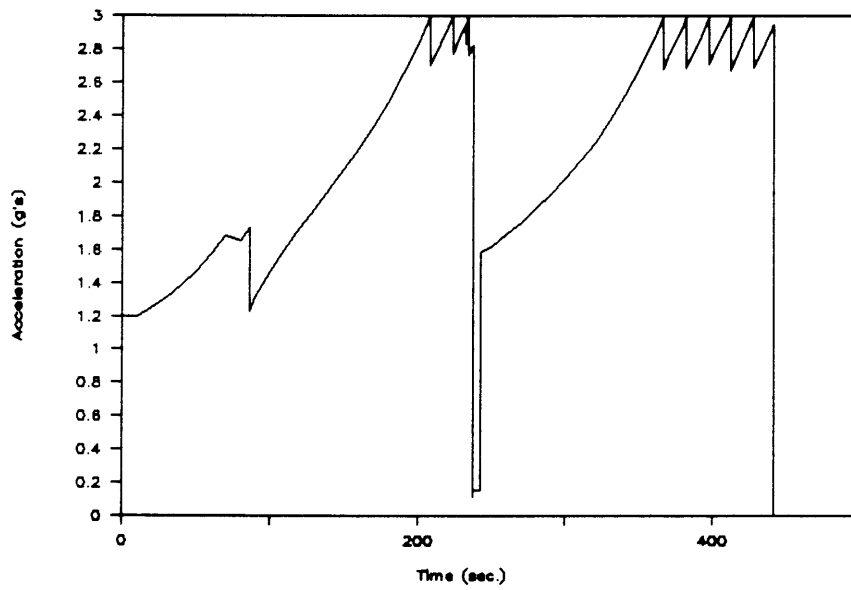


Figure 3.23: The perceived acceleration as sensed by the payload as a function of time.

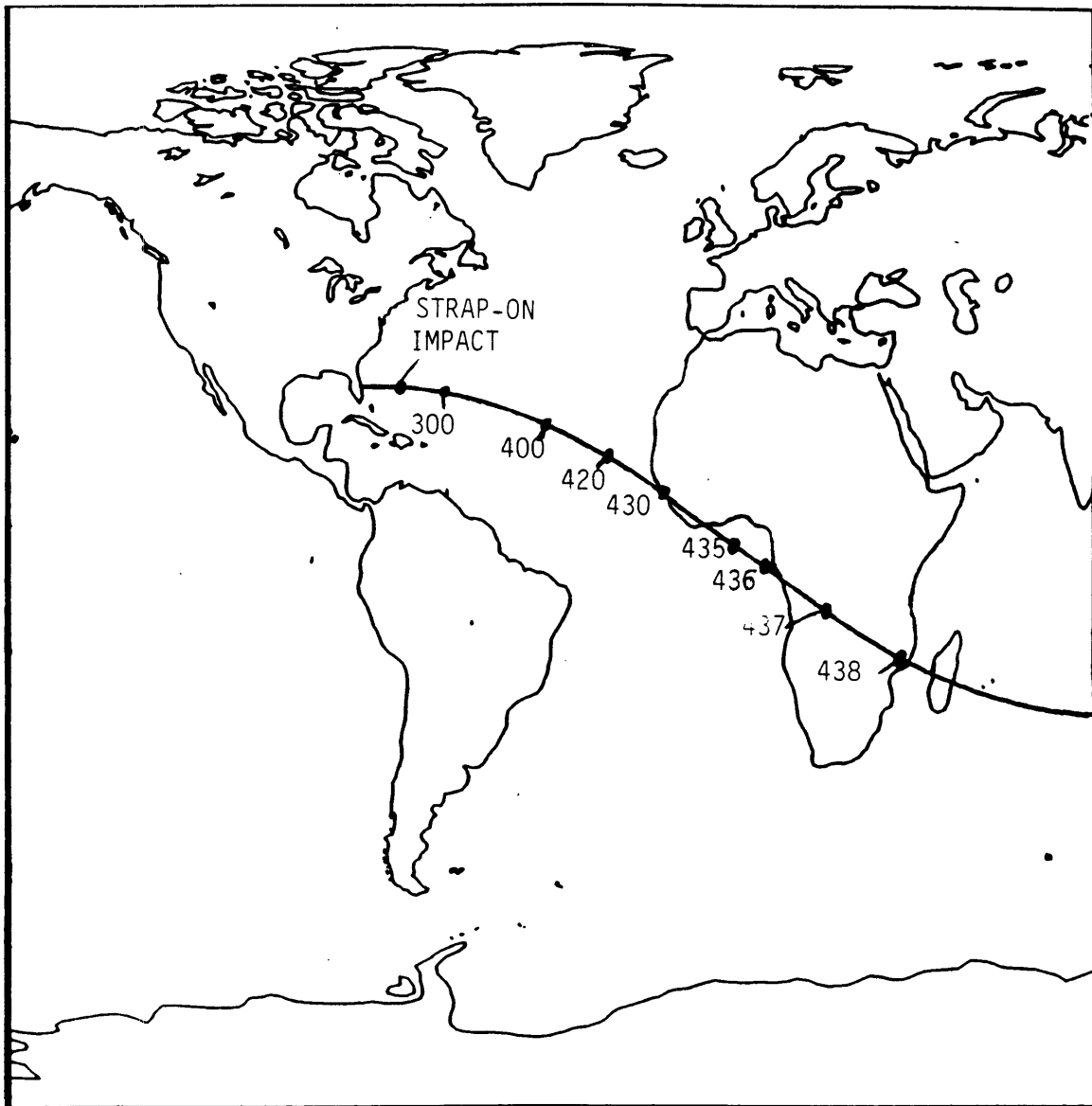


Figure 3.24: The vacuum instantaneous impact point of the launch vehicle at specific points in time.

Chapter 4

Engine Failure

4.1 Overview

Of the failure modes of a launch vehicle, the one that seems the most likely to occur on this vehicle is having an engine fail in flight. With 30 engines per strap-on, there will probably not be time to inspect every engine after each flight. When combined with the core engines, which presumably will have previously been flown on strap-ons, there are 318 engines, most of which have been used and few of which have been closely inspected since leaving the factory. Although these engines are simple enough to permit extensive qualification testing, the fact that there are 318 of them means that the possibility of an engine failing is higher than that of other launch vehicles. Further, since one is carrying 340,000 pounds of expensive payload, one must take steps to insure that an engine failure will not jeopardize the mission.

If an engine failure is fracticidal (that is, if the engine fails by exploding), then the launch vehicle will almost certainly be destroyed. The force of an engine explosion will rupture much of the rest of the vehicle. Fortunately, it is difficult for the RL10J to fail this way. Its simple design draws less and less propellant in the event of malfunction, virtually guaranteeing a safe shutdown. Further, the engine operates with comparatively low chamber pressure, guarding against some kind of

structural failure. For example, the RL10J operates at a pressure of 575 psi (3960 kPa) [2] where the Space Shuttle Main Engine operates at nearly 3000 psi (20,600 kPa) [1, page A-53].

If an engine failure is fratricidal (that is, if one engine failure causes the whole cluster to fail), then having a cluster, or clusters, out must be considered. Without examining plumbing and other possible failure modes, this type of failure seems more likely and more survivable than the fracticidal failure. Thus, this 'cluster out' will be investigated as well as a single engine out.

The first issue associated with engine failure is that of performance. Clearly, fewer working engines means less payload, but the question is how fast this performance falls off. The second issue is that of control authority. Having an engine out means asymmetric thrust, and this must somehow be corrected. Before calculating the control needed for correcting failed engines, one needs to calculate the control for the nominal case. The third issue is that of propellant management. When an engine fails on a strap-on, that strap-on will consume propellant more slowly, resulting in a longer burntime and uneven weight distribution. Each of these issues is addressed in a separate section below, along with a summary of conclusions.

4.2 Payload Capability

The payload capability of the vehicle with failed engines is dependent on the number and location of these engines. As can be seen in section 3.2.3 above, one would prefer to have as many engines on the strap-on as possible, so failed strap-on engines will have a more negative effect than failed core engines. Further, a failed engine early in the flight will have a more negative effect than a failed engine later in the flight. To carry out this analysis, a certain number of core and strap-on engines were assumed to be non-existent, equivalent to assuming that they had failed from launch and never work. The results are printed in the table below where, as above, LEO is an

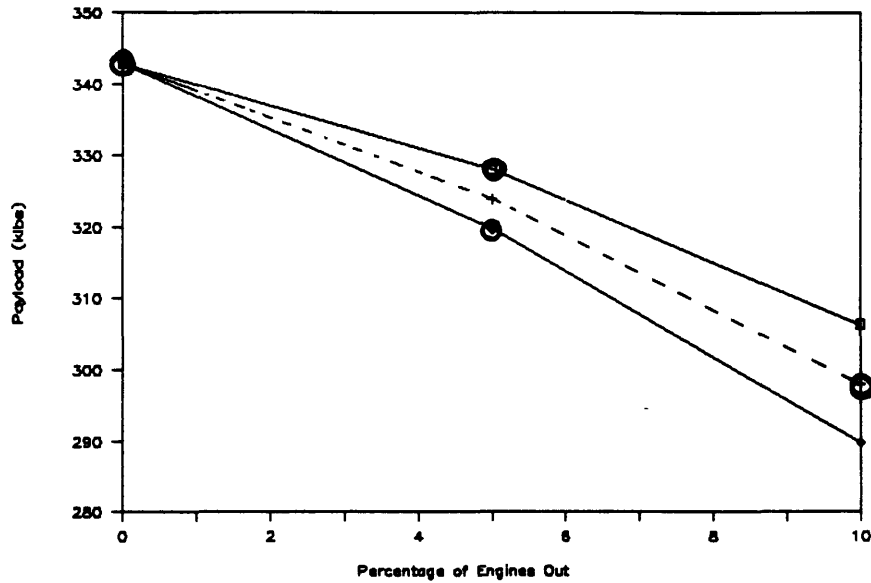


Figure 4.1: Loss of performance as a function of engine loss.

abbreviation for low Earth orbit.

Number of Core Engines Out	Number of Strap-on Engines Out (each)	Total Number of Engines Out	Payload to LEO (lbs)
0 (0%)	0 (0%)	0 (0%)	342,800
0 (0%)	2 (7%)	16 (5%)	319,700
8 (10%)	1 (3%)	16 (5%)	328,000
8 (10%)	3 (10%)	32 (10%)	298,100

Figure 4.1 shows the variation graphically. The lowest line is the 'worst case' payload capability: all of the failed engines are on the strap-ons. The dotted line is the payload if an equal percentage of core and strap-on engines have failed, and the uppermost line shows the payload if more core than strap-on engines have failed. The circled values were calculated above, and all others were extrapolated.

Note that the capability to handle failed engines must be selected in advance. For example, to handle a 10% engine out case, only 290,000 lbs of payload would be carried and the propellant and flight software would be loaded accordingly. If the vehicle is prepared for a specific failed engine capability and engines do not fail,

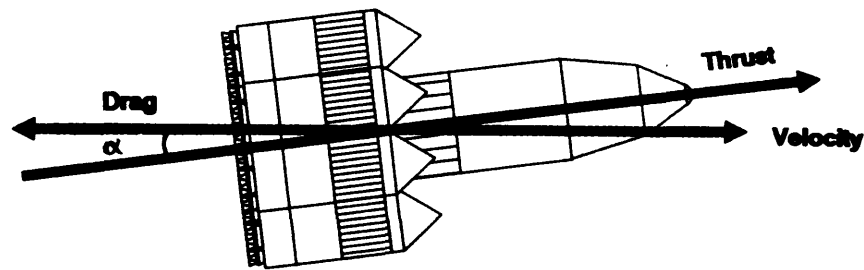


Figure 4.2: The geometry of the thrust, velocity, and drag vectors.

the vehicle can turn off engines deliberately, fly a non-optimal trajectory, cut off engines before all of the propellant is expended, or perform some combination of these strategies. This means that the customer can select the reliability of the launch vehicle in advance, as a higher failed engine capability means higher reliability but lower performance.

4.3 Control

Before calculating the control needed with failed engines, the control needed to handle a normal flight must be calculated.

4.3.1 Nominal Control

The most strenuous periods of control are accommodating a finite angle of attack when drag is at its peak and accommodating a wind gust when gusts are at their worst.

From the trajectory described above, the pitch angle is 3.9° from the flight path angle while passing through the maximum drag. Assuming that the thrust vector is aligned with the long axis of the vehicle, this means that the vehicle is travelling at a 3.9° angle of attack, as in figure 4.2.

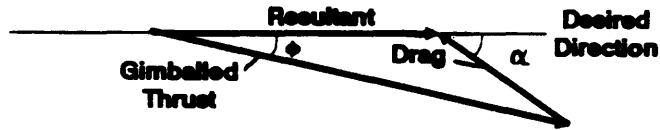


Figure 4.3: The gimbale angle ϕ required to cancel out drag at an angle of attack α .

This offset drag produces both a normal force and moment on the vehicle. The magnitude of the moment depends on the location of the center of pressure (the point where the drag can be considered to act), calculation of which is felt to be beyond the scope of this discussion. It is also noted that this non-zero angle of attack will increase the magnitude of the drag and induce lift. Calculation of these effects is also beyond the scope. For now, it will be assumed that the center of pressure of the launch vehicle is at or extremely close to the center of gravity, and that the drag is that calculated by the flight simulation. The gimbale angles will be those required to cancel out the normal force, as shown in figure 4.3.

This assumption yields

$$D \sin \alpha = T \sin \phi$$

or

$$\phi = \sin^{-1} \left(\frac{D}{T} \sin \alpha \right) \quad (4.1)$$

From the trajectory data at 86 seconds, drag is about 1506 klbs and the total thrust is 7850 klbs. Since each engine gimbals about only one axis, the thrust available for gimbaling is one-half of the total thrust, or 3925 klbs. This yields a gimbale angle of 1.6° .

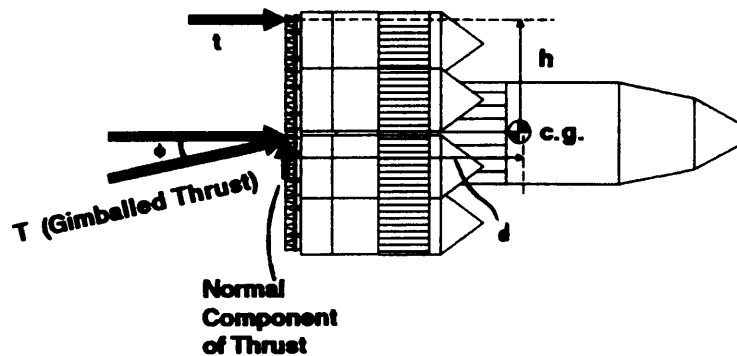


Figure 4.4: Geometry of an engine out and the corrective moments.

The worst case gust loads occur at 43,000 ft, where the 95 percentile wind with embedded gust is 270 ft/sec [5, page 19]. The vehicle is already at a 4.2° angle between the thrust and velocity, and the 270 ft/sec gust on a vehicle travelling at 1350 ft/sec results in a 15.5° total angle between thrust and drag. This number is excessively high; it must be remembered that this is only an instantaneous angle of attack but this does show that these gusts will produce severe forces on the launch vehicle. Using equation 4.1 and the trajectory data at 90 seconds, one obtains a total gimballed angle of 5.0° . Thus, gusts are three times as stringent as simple angle of attack.

4.3.2 Control with Failed Engines

A failed engine creates a moment which must be corrected by the remaining engines. The lack of thrust at a point can be thought of as an unbalanced thrust at the opposite point. The geometry of the moments involved is shown in figure 4.4.

The basic equation dictating the gimballed angle is a moment balance, as follows.

$$Td \sin \phi = th$$

or

$$\phi = \sin^{-1} \left[\left(\frac{t}{T} \right) \left(\frac{h}{d} \right) \right] \quad (4.2)$$

as expressed in dimensionless groupings.

The first item to be calculated is d , the height of the center of gravity. For this calculation, it was assumed that the weight of each engine is 450 lbs [2], centered three feet below the base of each core and strap-on. The remainder of the inert structural weight was assumed to be centered exactly halfway between the base and the top of each module. The location of the center of gravity was calculated without any propellant and then with a full load of propellant. It was then assumed that the location of the center of gravity changed linearly with propellant consumption. Given all of these assumptions, the center of gravity was calculated to be 49.8 ft above the base of the core at 90 seconds into the flight. All subsequent calculations also assume parameter values at 90 seconds into the flight.

Single Engine Out

Assuming an outboard engine has failed, h is the radius of the core plus the diameter of a strap-on, or 47.2 ft. There are 239 other engines operating, as the core is shut down. Taking into account single-axis gimbaling, there are 239/2 engines available to correct the 1 engine out. Thus

$$\phi = \sin^{-1} \left[\left(\frac{2}{239} \right) \left(\frac{47.2}{49.8} \right) \right] = 0.5^\circ$$

Single Cluster Out

A cluster has a width of 5 ft and is located slightly inboard from the booster edge, so h is 44 ft. There are 234/2 engines available to correct for the 6 engines out. Thus,

$$\phi = \sin^{-1} \left[\left(\frac{12}{234} \right) \left(\frac{44.0}{49.8} \right) \right] = 2.6^\circ$$

A second cluster out will have less than double the effect, as any other cluster out will decrease h .

Booster Out

Just to study an extreme case, the gimballed angle required to correct for an entire booster being out will be calculated. The 10% engine out case above has 32 failed engines, so a booster out can be handled propulsively.

In this case, h is the radius of the core plus the radius of a strap-on, or 34.1 ft. There are 30 engines out and 210/2 left to steer. This yields

$$\phi = \sin^{-1} \left[\left(\frac{60}{210} \right) \left(\frac{34.1}{49.8} \right) \right] = 11.3^\circ$$

This, when combined with the gust loads, would be difficult to accommodate.

4.3.3 Control Summary

To handle worst-case gusting and a cluster out on one side, the engines need to gimbal eight degrees. This gives a thrust cosine loss of 1%, equivalent to an additional two engines out in a propulsive sense. Handling a booster out would require sixteen degrees of gimballed angle, which is felt to be excessive. If more than one cluster goes out, they need to be far apart from one another if the vehicle is to maintain control. While one can accommodate up to 5 clusters out propulsively, they cannot necessarily be accommodated by the control system, so some engineering should go into preventing fratricidal engine failures.

The two methods that could circumvent the need for gimbaling are injection and control fins. Injection is a method that injects propellant into the nozzle, resulting in asymmetric thrust. Control fins are vanes located at the base of the launch vehicle that act as control surfaces, similar to control surfaces on aircraft. Use of either of these methods could reduce or eliminate the need for gimbaling.

4.4 Propellant Consumption Management

Another problem with failed engines is that it means that some strap-ons will consume propellant slower than other strap-ons, leading to different burnout times and accentuating the problem of unequal thrust with unequal weight. Several methods for correcting this are discussed in a qualitative fashion below.

The most effective and the most complicated method for assuring equal propellant consumption is to crossfeed propellant between the strap-ons. This will guarantee simultaneous burnout and will, with the use of controllable valves, allow one to control the weight of propellant in each strap-on. The disadvantage of this scheme is that it greatly increases the cost and complexity of an already complicated propellant feed system, as well as giving the avionics system one more parameter to control.

A simple way of correcting consumption is to be careful in selecting which engines are shut down to limit acceleration. In the baseline case, seven engines have been shut down on each strap-on at the time they burn out. If none of the functioning engines are shut down on the defective strap-on, and if the only engines that are shut down are on the working strap-ons, this would allow the defective strap-on to 'catch up' in fuel consumption. The problem with this scheme is that it is time-limited. Suppose an engine fails at launch. No further engines are shut down until 208 seconds, and burnout occurs at 237 seconds. The 29 seconds of unequal engine shut down is not enough time to catch up to the 208 seconds of a single failed engine. This scheme can help other schemes, but it is not enough in itself to correct the problem.

Another method for changing the thrust as well as the burnout time is to adjust the engine burn parameters, e.g. the hydrogen/oxygen mixture ratio. This could either accentuate or alleviate the unequal thrust of the failed engine, as the new burn parameters will result in a different thrust. By altering the mixture ratio, the defective strap-on could be made to burn faster and so keep up with the working

strap-ons. However, this means more extensive engine testing, hardware, and flight software and increases the cost and complexity of the engines.

The simplest method of equalizing both thrust and consumption is to shut down an engine on each strap-on when one fails on a single strap-on. This method is guaranteed to equalize all of the strap-ons, thus alleviating the need for gimbaling. However, this multiplies the effect of an engine out by a factor of eight.

Overall, then, a strategy employing crossfeeding appears to be too cumbersome and expensive. This should only be used if it appears that multiple engine failure is fairly likely. Some combination of the other strategies can be used without drastic effects on normal performance. For example, a single engine out at liftoff could be alleviated by turning off one engine on each strap-on just after passing through the maximum gust zone. As g-limits are encountered, no further engines are turned off on the defective strap-on until the propellant loading is equalized. The strategies employed become more complicated with increasingly complex scenarios, as when engines fail at various points in the flight. Some detailed study would need to be done in this area, and the results would be incorporated into the flight software.

4.5 Engine Failure Summary

From a propulsive standpoint, engine failure can be accommodated simply by launching with less than the maximum amount of payload and using a non-optimal trajectory if no engines fail. From the standpoint of controls, an eight degree engine gimbal capacity can insure vehicle control during maximum gusts with an outboard cluster out. Whether the vehicle can handle more engines out depends on where these engines are located. Use of fins or injection techniques can increase the available control authority. From a propellant standpoint, the vehicle will have to shut down or throttle down engines on the fully functioning strap-ons in order to even out propellant consumption. A shutdown could take part as normal acceleration

limitation or as a premature shutdown. The throttling down could be carried out by varying the propellant ratio.

Engine failure, then, can be credibly handled by gimbaling and engine shutdown, leading one to conclude that an engine failure will not jeopardize the mission.

Chapter 5

Conclusion

The goal of this study has been to demonstrate that one does not need to use complex and expensive rocket engines in order to deliver large amounts of payload to low Earth orbit. A design using over 300 small engines was derived by using the rocket equations to determine propellant capacity and using this capacity to size the propulsion system, strap-on boosters, and propellant tanks.

This initial design, featuring 78 engines placed on a 42 ft diameter core and eight 26 ft diameter strap-ons with 30 engines apiece, was then refined by varying five design parameters and selecting values which maximized payload capacity within constraints. These parameters were liftoff mass, core/strap-on size ratio, core/strap-on engine ratio, acceleration limit, and core shutdown time, and constraints included takeoff thrust/weight ratio, space for the engines to gimbal, and time of maximum dynamic pressure. The most interesting of these studies was the variation in acceleration limit. This scheme is made possible by the large number of engines, allowing one to precisely control the thrust by shutting down engines as needed. The payload capability is virtually a constant when the limit is over 2.5 g's.

Next, several externally determined vehicle parameters were varied to determine the effect on payload capacity if these parameters have unexpected or non-ideal

values. These parameters included mass fraction, drag, number of strap-ons, and specific impulse. The payload capacity was strongly dependent on specific impulse and mass fraction, but weakly dependent on drag. The variation in number of strap-ons showed that the highly modular eight strap-on approach resulted in a wide range of payload capability with the same design.

The increased likelihood of engine failure is somewhat alleviated by the inherent reliability and robustness of the engine design. Nevertheless, analysis showed that the vehicle can carry a fairly large amount of payload even with 10% of the engines out from liftoff. Further, an 8° engine gimbal capacity insures control with one failed cluster of six engines during maximum gusts, and this control authority can be augmented by other techniques, such as fins. Several methods of propellant consumption management were discussed that could alleviate the problem of unequal propellant consumption when engines have failed. Some combination of these methods would control consumption with minimal impact on the nominal system.

In summary, the design is based on engine technology that is decades old, but it can deliver many times the payload of existing launchers. The customer can select the acceleration limit (as low as 2.0 g's) and the failed engine capacity (as high as 10% of the engines failed at liftoff), which are two features that no existing launchers can offer. Further, the same basic design can carry anywhere from 40,000 to 340,000 lbs to low Earth orbit. The result is a very capable, flexible, and reliable design.

Bibliography

- [1] Space Systems Engineering Class. *Design of a Mixed Fleet Transportation System to Low Earth Orbit*, Volume 3. Department of Aeronautics and Astronautics of Massachusetts Institute of Technology, Cambridge, MA. Spring, 1987.
- [2] Brown, J. R. *RL10J Propulsion Status Presentation at Hughes ALS Design Study In-Plant Review*. August 13, 1987
- [3] Hill, P. G. and Peterson, C. R. *Mechanics and Thermodynamics of Propulsion*. Addison-Wesley Publishing Company, Reading, MI. 1970.
- [4] Battin, Richard H. *An Introduction to the Mathematics and Methods of Astrodynamics*. C. S. Draper Laboratory, Cambridge, MA. 1986.
- [5] Toelle, R. (ed.) *Heavy Lift Launch Vehicles for 1995 and Beyond*. NASA Technical Memorandum TM-86520. National Aeronautics and Space Administration, Washington, D.C. 1985.
- [6] *Titan III Commercial Launch Services Payload Users Handbook*. Martin Marietta Denver Aerospace, Denver, CO. 1986.
- [7] *Atlas H and K Vehicle System Mission Planners Guide*. General Dynamics Convair Division, San Diego, CA. 1984.
- [8] *Ariane 4 User's Manual*. Arianespace, Evry, France. 1983
- [9] Flügge, W. *Stresses in Shells*. Springer-Verlag, Berlin, Germany. 1962.